Stiffness-based approach for Belleville springs use in friction sliding structural connections

Article in Journal of Constructional Steel Research · November 2017

DOI: 10.1016/j.jcsr.2017.07.009

4 authors:

Shahab Ramhormozian
Auckland University of Technology

George Charles Clifton
University of Auckland

Gregory A. Macrae
University of Canterbury

George P. Davet
Solon Manufacturing Company

Post-print/not finalized

Title: Stiffness-Based Approach for Belleville Springs use in Friction Sliding Structural Connections

Authors: Shahab Ramhormozian[a,*], G. Charles Clifton[a], Gregory A. MacRae[b], George P. Davet[c]

[*]Corresponding Author: Shahab Ramhormozian

[a] *Department of Civil and Environmental Engineering, University of Auckland, Engineering Building, 20 Symonds Street, Auckland, New Zealand*

[b] *School of Civil and Natural Resources Engineering, The University of Canterbury, Christchurch, New Zealand*

[c] *Solon Manufacturing Company, Cleveland, Ohio, USA*

Shahab Ramhormozian: Department of Civil and Environmental Engineering, University of Auckland, Engineering Building, 20 Symonds Street, Auckland, New Zealand
Email: sram732@aucklanduni.ac.nz

G. Charles Clifton: Department of Civil and Environmental Engineering, University of Auckland, Engineering Building, 20 Symonds Street, Auckland, New Zealand
Email: c.clifton@auckland.ac.nz

Gregory A. MacRae: School of Civil and Environmental Engineering, The University of Canterbury, Christchurch, New Zealand
Email: gregory.macrae@canterbury.ac.nz

George P. Davet: Solon Manufacturing Company, Cleveland, Ohio, USA
Email: gdavet@solonmfg.com

Shahab Ramhormozian: MSc, PhD Student

G. Charles Clifton: PhD, Associate Professor

Gregory A. MacRae: PhD, Associate Professor

George P. Davet: BSME, Chief Engineer

Stiffness-Based Approach for Belleville Springs use in Friction Sliding Structural Connections

Sliding hinge joints (SHJs) used in beam-to-column connections of moment frames have a moment-rotational behaviour that depends on asymmetric friction connection (AFC) sliding behaviour. The AFC is also applied to column base connections and friction sliding braces. In the AFC, the slotted sliding plate is clamped between one ideally fixed surface and one partially floating surface. In current practice, the AFC bolts are fully tensioned at installation (i.e. yielded) to provide the clamping force. The AFC bolts are subjected to moment, shear, and axial force (MVP) interaction during joint sliding that is expected to occur only in severe earthquake shaking. The AFC bolt tension as well as SHJ elastic strength are reduced after a few sliding cycles. In this paper, the reasons for the AFC bolt tension loss are discussed, and solutions to prevent this bolt tension loss, including the optimum use of Belleville springs (BeSs) and installing the bolts within the elastic range, are proposed. This paper analytically shows that these solutions can generate significantly improved retention of AFC bolt tension, improved AFC sliding behaviour, higher displacement capacity to accommodate prying effects, and better AFC self-centring characteristics. Examples of AFC bolt installation within elastic range and tension loss with and without BeSs are provided. Similar models are developed for symmetric friction connections (SFCs) and compares differences in behaviour.

Keywords: Sliding hinge joint, Friction sliding connection, Earthquake, Low damage, Belleville spring, Bolt tension loss

1. Introduction

Although capacity-designed strong-column weak-beam steel moment resisting frames (MRFs) have performed well in past earthquakes, with no reported collapses and loss of life related to these structural systems, their performance has not always been fully as expected in severe earthquakes. Observed fractures at welded moment connections in the 1994 Northridge Earthquake [1] and the 1995 Kobe Earthquake [2] showed weaknesses of the steel MRFs, where many traditional rigid welded steel connections suffered unexpected fracture, mostly in the beam bottom flange to column flange welds. These partial failures did not lead to building collapse, and showed that the change in behaviour from rigid connections to strong column weak beam semi-rigid connections can, for the overall structural system, deliver satisfactory life safety seismic performance.

The basic shortcoming of beam-to-column connections in steel MRFs experienced in the 1994 Northridge and the 1995 Kobe Earthquakes [3] led to the development of methods to avoid weld failure in steel connections. These methods, such as the reduced beam section and bolted flange plate connections [4] are still based on the capacity design philosophy, where the plastic demand is confined to predetermined regions to provide safety and prevent collapse. However, these systems are typically associated with plastic deformation in the beams or joints, hence potentially impose large economic losses in the post-disaster repair and downtime due to closure of the building [5]. These economic issues have been underlined in recent severe earthquakes such as the 1994 Northridge, 1995 Kobe, 2010/2011 Christchurch, and 2016 Kaikoura earthquakes. Consequently there is now an increasing emphasis on developing and implementing low damage seismic resisting systems, to make the building operational rapidly or, ideally, immediately after a severe earthquake. Two examples of such low damage systems are rotational slotted bolted connection (RSBC) [6] using symmetric friction connections (SFCs), and Sliding Hinge Joint connection (SHJ) [7] using Asymmetric Friction Connections (AFCs). SFC and AFC are friction seismic energy dissipating components of the RSBC and SHJ respectively.

Friction seismic energy dissipaters (dampers) have been researched for several decades (e.g. [8-11]). The slotted bolted connection (SBC) is a friction damper that dissipates energy through sliding between the interfaces of clamped-by-bolt metal plates, providing a non-linear inelastic behaviour. The sliding occurs at a predetermined sliding force related to the interfaces' coefficient of friction and the amount of clamping force. The SBC can be either SFC or AFC. The SFC (figure 1) consists of a middle plate (or outer plates) with slotted holes, sandwiched by (or sandwiching) two shims and two outer plates (or a middle plate) with circular holes, all clamped by bolts. Researchers (e.g. [12-16]) have experimentally researched the impact of different shim materials, such as mild steel, high hardness steel, brass, brake lining pad, stainless steel, aluminium, and rubber for SFC and/or AFC, with various results.

Yang and Popov [6] proposed and experimentally tested the RSBC which was a beam-column moment-resisting connection (figure 2) with two equal-capacity SFCs at the beam top and bottom flange levels. The SFC has also been experimentally researched to be used in other seismic structural systems such as post-tensioned steel tendon beam–column connections, steel braces with and without post-tensioning, eccentrically braced frames (EBFs) with rotational slotted bolted active link, and at the base of rocking timber shear walls, all showing reliable behaviour under seismic actions [17-26].

The AFC was originally proposed for the SHJ [27]. The SHJ is a low damage alternative to traditional beam-column connections for seismic MRSFs, and has been used in a number of multi-story buildings in New Zealand. The SHJ allows large beam-column relative rotation through sliding in two AFCs which are located at the beam web bottom bolt and bottom flange levels, as shown in Figure 3. The cleat has elongated holes to allow sliding, with standard sized bolt holes in the other AFC plies. The SHJ is ideally intended to: (i) be rigid under serviceability limit state (SLS) conditions, (ii) become semi-rigid allowing beam-column relative rotation to occur in ultimate limit state (ULS) and larger earthquakes through AFCs sliding and, (iii) seize up and become rigid again at the end of the earthquake. The AFC high strength friction grip (HSFG) property class (PC) 8.8 bolts are currently fully tensioned in practice at installation (i.e. yielded) with the part-turn method of tensioning in accordance to the New Zealand Steel Structures Standard, NZS 3404 [28]. The AFC has also been researched to be used at the column base and brace [29-31].

Both AFC and SFC have been shown experimentally by researchers to be degraded following a few cycles of sliding, meaning that the clamping force is reduced as a result of the bolts tension loss (e.g. [5, 6, 11, 27, 32-38]). This also has been shown numerically for the AFC through the finite element analysis [27, 39]. Although a repeatable stable sliding behaviour over many cycles is experimentally achievable, for example, for the AFC, the aforesaid degradation may affect the post sliding behaviour of the connection and building, by lowering the threshold of joint sliding in subsequent events or even in post-earthquake severe wind events. While these researchers generally reported improved seismic behaviour for the experiments using Belleville springs (BeSs), a conical washer type spring, and recommended using BeSs, for example, to maintain the post-sliding strength of the AFC [5, 27, 32, 33, 38] and/or SFC [6, 11, 34-36], there is not a conceptual detailed discussion found in the literature about the effect of using BeSs on the AFC and SFC seismic behaviour as well as the optimum procedure for using the BeSs.

To explain and justify more in depth the results of the undertaken experimental and numerical research in the field to date (e.g. [6, 11, 27, 32-39]) and to provide an essential base to the experimental and numerical research on the optimum use of BeSs in friction sliding structural connections as well as the practical design and optimum use of them, this paper seeks to provide analytical answers to the following questions:

1- What are the AFC and SFC sliding behaviours and what are the AFC and SFC post-sliding bolt tension loss reasons?

2- How can the compound stiffness of the AFC and SFC components i.e. the bolts, plies, and Belleville Springs (BeSs) be determined?

3- How can BeSs installed in the AFC and SFC bolt assemblage efficiently compensate for most of the post-sliding bolt tension loss?

4- How can BeSs be installed to improve the AFC self-centering capability and to prevent the AFC and SFC bolts plastic elongation due to the potential prying actions?

5- What are the other potential benefits of using BeSs in the AFC and SFC?

Finally a step-by-step design procedure for using BeSs in the AFC and SFC is proposed.

2. Asymmetric and symmetric friction connection sliding behaviour and bolt tension loss reasons

Figure 4 (a) shows the typical layout of an AFC with three rows of bolts at the SHJ beam bottom flange level. The AFC has two main sliding interfaces. The first is the interface between the cleat and the upper shim, and the second is the interface between the cleat and the lower shim. Figure 4 (b) shows the idealised force-displacement behaviour of the AFC. The sliding of the system commences when the applied force overcomes the frictional resistance of the first AFC sliding interface. After a relatively short distance of sliding, the second interface also starts to slide, pushing the AFC bolts into the double curvature state named as stable sliding state. Upon load reversal, the same behaviour is attained but in the opposite direction. This AFC behaviour is resulted from the AFC having a partially floating cap, and provides the SHJ, or any system incorporating the AFC, with a “pinched” hysteretic curve, which is closer to a flag-shaped hysteresis curve, compared with the square curve of a SFC assemblage and hence is desirable from the self-centring point of view.

The SFC force-displacement behaviour is simpler than the AFC's. The two main sliding interfaces of the SFC are between the middle plate and upper and lower shims (figure 1) or between the outer plates and upper and lower shims as well as under the bolt head and nut, if the slotted holes are in the outer plates. When the applied force overcomes the frictional resistance of both SFC sliding interfaces, the sliding of the system commences while the bolts are ideally, only under the tension for the SFC with slotted middle plate and under the tension, shear, and bending moment for the SFC with slotted outer plates. This provides the SFC with an idealized rectangular hysteretic curve (Figure 1).

The AFC and SFC are subject to a post-sliding elastic strength reduction due to bolt tension loss which may cause the AFC and SFC to commence sliding at a less intense subsequent excitation. This is because:

I. When the AFC (or the SFC with outer slotted plates layout) starts to slide, the bending moment induced tensile stress, the additional tensile stress in the bolt, and the shear stress combine with the high bolt installed tensile stress to further plasticize the bolt. As the fully tensioned bolt is expected to be yielded at installation, it undergoes further local plastic action under a small increase particularly in tensile stress over the part of its cross section, where the bending induced stress is tensile. In addition to the connections geometry, the coefficient of friction as well as the clamping force are the influential parameters on this MVP interaction according to the plastic theory based AFC bolt model [40]. Given the "back and forth" nature of the earthquake resulted building response, this may affect a large part of the bolt cross section, resulting in a post sliding AFC bolt plastic elongation [27, 39, 41]. In a set of non-prying AFC sliding experiments undertaken by Ramhormozian, Clifton et al. [38] in which the ¾ inch imperial black bolts of property class 10.9 were installed to a tensioned range of 30% to 60% of their proof load, an average post-sliding AFC bolt plastic elongation (of total bolt length) of about 0.04mm is measured. Figure 5 shows the AFC idealised bolt deformation, external forces, and bending moment distribution. It was shown numerically [27, 39] through the finite element modelling of a SHJ beam bottom flange AFC bolt that the MVP interaction has a significant effect on the bolt tension loss, resulting in a stable sliding bolt tension of 55% and 60% of the installed bolt tension of the fully tensioned HSFG PC8.8 M24 and M30 bolts respectively, after two loading cycles. This numerical study did not consider the prying actions and the AFC plies post sliding thickness reduction, which are explained in parts II and III below.

II. The cleat prying may potentially further plasticize the AFC bolts during sliding by imposing a high extra tensile strain on the bolt [5, 32, 41]. This is the case for the AFC and SFC bolts where they may be subjected to prying forces depending on the system boundary conditions, for example, for the AFC bolts at the beam bottom flange level of the SHJ. This may be influenced by the cleat and beam flange thickness, SHJ beam-column initial gap, SHJ beam column relative rotation, level of the AFC bolts tension, size of the AFC bolts, number of AFC bolt rows, and geometrical characteristics of the connection.

III. Due to the clamping force generated by the AFC and SFC bolts, localized bearing stresses can reduce the total thickness of the AFC and SFC plates and shims per bolt during the time of sliding and even over the time without sliding [36, 38]. Yielding of the microscopic high spots on the AFC sliding surfaces and changing the locations of contact points "points at which two surfaces are in contact" of the AFC and SFC sliding surfaces can occur. Figure 6 shows surface roughness, waviness, and microscopic high spots on a schematic sliding surface. Yielding of the high spots will decrease the surface roughness while changing the locations of contact points can face one surface waviness peak with another surface waviness valley. Additionally it has been experimentally shown that removal of material from solid sliding surfaces (i.e. wearing) occurs for both AFC and SFC during sliding [6, 16]. As a result, the AFC and SFC plies' thickness reduces following a few cycles of sliding, hence the grip length being clamped by the bolt shortens [32, 38], causing a drop in the bolt tension. Ramhormozian, Clifton et al. [38] experimentally measured an average post sliding reduction in the total ply thickness of 0.1mm per AFC bolt for a set of experiments in which the ¾ inch diameter imperial black bolts of property class 10.9 were installed to a tensioned range of 30% to 60% of their proof load.

IV. AFC and SFC bolts can potentially rub against sides of the slotted holes resulting in a shear force imposed on the bolts and reducing their integrity. This may potentially occur, for example, for the SHJ's AFC at beam web bottom bolt level or for the AFCs and SFCs in the braces with long slotted holes and potential long sliding travels not perfectly aligned with the slotted holes.

V. Similar to any other type of bolted connection, AFC and SFC bolts may be susceptible to the tension loss due to the factors such as short term and long term bolt relaxations, joint creep, and vibration induced bolt self-loosening.

Sections 3, 4, and 5 describe formulating the bolt, joint's plies, and BeSs stiffness values which are required to model the AFC's and SFC's pre and post sliding conditions that are described in section 6.

3. Bolt longitudinal stiffness:

The bolt longitudinal stiffness can be determined by considering the bolt as a set of spring systems, namely the bolt's 1) head, 2) shank, 3) threaded portion between the shank and nut underneath, and 4) threaded portion engaged with the nut, along with the nut (Figure 7). These parts contribute in carrying the bolt pretension load when a bolt is tightened.

3.1. Bolt shank longitudinal stiffness:

Assuming the bolt is behaving in the elastic range and considering the Hooke's law, the bolt shank longitudinal stiffness, K_s, can be calculated by Equation 1:

$$K_s = \frac{F}{\Delta L_s} = \frac{\iint \sigma_{xx} dA}{\int_0^{L_{0s}} \frac{\sigma_{xx}}{E} dx} = \frac{\sigma_{xx} A_{0s}}{\sigma_{xx} \frac{L_{0s}}{E}} = \frac{A_{0s} E}{L_{0s}} \tag{1}$$

where F=axial tensile force applied on the bolt, equal to the connection plies clamping force per bolt; ΔL_s=shank elongation due to applied F; σ_{xx}=uniformly distributed tensile stress on the shank cross section due to applied F; E=elastic modulus of the bolt material; A_{0s}=initial shank cross sectional area i.e. before applying the force F; L_{0s}=initial shank length. Equation 1 is in agreement with the value presented in [42].

3.2. Bolt threaded part longitudinal stiffness:

Similarly, the longitudinal stiffness of the bolt threaded portion between the shank and nut underneath, K_t, can be calculated by Equation 2:

$$K_t = \frac{A_{0t} E}{L_{0t}} \tag{2}$$

where A_{0t}=initial bolt thread stress area; L_{0t}=initial length of the bolt threaded portion between the shank and nut underneath. Equation 2 is in agreement with the value presented in [42].

3.3. Bolt engaged-with-the-nut threaded part, along with nut longitudinal stiffness:

Experiments have shown that to take the bolt engaged threads elastic deformation into account, a length of $0.4D_{0s}$ needs to be added to the joint grip length in the bolt longitudinal stiffness calculations [42, 43], where D_{0s}=initial bolt shank diameter. The values from $0.3D_{0s}$ to $0.6D_{0s}$ have also been suggested by different sources [42]. Bickford [44] suggests a value of $0.5D_{0s}$ for this contribution. To determine analytically the longitudinal stiffness of the bolt threaded portion which is in contact with the nut, it is necessary to determine the load distribution along the bolt threads which are in contact with the nut threads. This load distribution is not uniform, as the nut and threaded portion both have elastic flexibility. Most of the applied load is carried by the first three engaged threads, and the load distribution depends upon a number of parameters including the form of threads, the thickness of the walls supporting the threads at the threaded section, the pitch of the threads, the number of engaged threads, and the boundary conditions [45].

An analytical theory to predict the load distribution in bolt threads in contact with the nut threads was suggested by Sopwith [46]. Miller, Marshek et al. [47] developed a model for predicting this load distribution using second order difference equations. Their model consisted of a set of elastic elements "springs" to represent the main body, as well as threads of the bolt and nut. They verified their theory by comparison with finite element analysis results, as well as with previous experimental and analytical investigations of threaded connections. Wang and Marshek [48] developed a modified spring model similar to the model proposed by Miller, Marshek et al. [47] to predict the load distribution in the bolt threaded portion which is in contact with the nut threads. They also took yielding of the threads into account. They concluded that the lower number threads always carry a higher load, and when these threads yield, the next unyielded threads will carry a greater load as the bolt preload increases.

Based on an example described in [48] for the steel bolt with 25.4mm diameter and 8 engaged Whitworth threads, there is an agreement between finite element, spring, photo-elastic, and Sopwith analytical models of the bolt threaded portion in contact with the nut threads to predict the load distribution over the bolt and nut engaged threads, although the finite element model predicts a slightly higher value for the load on the first thread. These results are for the case named as compression case (or nut and bolt case), in which the boundary conditions are the same as the AFC and SFC bolts assemblages. These results predict the load applied on each one of the bolt threads engaged with the nut threads.

By adopting the results of the comparison carried out by Miller, Marshek et al. [47] and Wang and Marshek [48] between different modelling methods, this paper proposes the load distribution into the threads given in Table 1. This table gives the predicted value of the applied force at certain points of the bolt threaded portion engaged with the nut threads, with a specific distance from the nut underneath. These values are then used to discretize the integration presented in Equation 3, and can be used for any steel bolt size, nut thickness, and number of engaged bolt threads with the nut threads, to estimate the load distribution along the bolt engage-with-the-nut and nut threaded parts. This table is based on the bolt being tensioned into the elastic range up to the point that the most heavily loaded thread i.e. the lowest thread, starts to yield. Figure 8 schematically shows this load distribution.

Equation 3 is used to calculate the elongation of the bolt threaded portion which is in contact with the nut, (ΔL_{tnb}), due to an arbitrary bolt preload F.

$$\Delta L_{tnb} = \int_0^{H_{0n}} \frac{F(x)}{A_{0t}E} dx \cong \sum_{i=1}^{8} \frac{F_i(x)}{A_{0t}E} \Delta x_i = \frac{0.125 H_{0n}}{A_{0t}E} \sum_{i=1}^{8} F_i(x)$$

$$= \frac{0.125 H_{0n}}{A_{0t}E} \times \frac{F}{100} \times (0 + 3.5 + 8.5 + 14.5 + 22.5 + 33 + 47.5 + 69) \qquad (3)$$

$$= \frac{0.25 H_{0n} F}{A_{0t} E}$$

where H_{0n}=nut initial height i.e. before being compressed; $F(x)$=load function representing the axial tensile load applied on the bolt engaged threaded part's cross section, at the point with distance x from the nut underneath.

The longitudinal stiffness of the bolt threaded portion which is in contact with the nut is calculated by Equation 4.

$$K_{tnb} = \frac{F}{\Delta L_{tnb}} = \frac{A_{0t} E}{0.25 H_{0n}} \tag{4}$$

Similarly, the nut stiffness, K_{tnn}, is calculated by Equation 5.

$$K_{tnn} = (A_{0n}/A_{0t}) K_{tnb} = \frac{A_{0n} E}{0.25 H_{0n}} \tag{5}$$

where A_{0n}=nut initial cross sectional stress area.

The bolt threaded part and nut together can be considered as two springs in series. As the bolt is tightened, a load equal to the bolt preload is applied at the nut underneath, the bolt threaded part is tensioned, and the nut is compressed, both based on the load distribution shown in Figure 8. The overall cumulative deflection is the summation of these two deflections, as it is assumed that there is no force transferred between the far end (unloaded face) of the nut threaded portion and the bolt threaded portion, hence there is no relative displacement. One can assume a dummy rigid bar at the unloaded face of the nut to model this behaviour, as is shown schematically in Figure 7. Hence, the overall stiffness of the bolt threaded portion engaged with the nut, along with the nut itself, K_{tn}, can be calculated by Equation 6.

$$K_{tn} = \frac{1}{\frac{1}{K_{tnb}} + \frac{1}{K_{tnn}}} = \frac{K_{tnb} K_{tnn}}{K_{tnb} + K_{tnn}} = \frac{A_{0n} A_{0t} E}{0.25 H_{0n} (A_{0n} + A_{0t})} = \frac{(A_{0n}/A_{0t}) K_{tnb}}{1 + (A_{0n}/A_{0t})} \tag{6}$$

3.4. Bolt head longitudinal stiffness:

To take the bolt head elastic deformation into account, which is conceptually similar to the elastic deformation of the bolt engaged-with-the-nut threaded part and nut, VDI 2230 [43] suggests a length of $0.4D_{0s}$ be added to the joint grip length in the bolt longitudinal stiffness calculations, where D_{0s}=initial bolt shank diameter. Bickford [44] suggests a value of $0.5D_{0s}$ for this bolt head contribution. Alkatan, Stephan et al. [49] proposed an equation to calculate the length for the bolt head contribution. This equation is related to the bolt geometry, bolt and fastened plies materials, and the coefficient of friction between the bolt head underneath and the fastened ply.

By adopting the equation proposed by Alkatan, Stephan et al. [49], this paper proposes Equation 7 to calculate the bolt head longitudinal stiffness, K_h. Equation 7 considers the same elastic modulus for the bolt and joint plies materials, standardized head height of $0.65D_{0s}$, and the coefficient of friction of 0.2 for the bolt head underneath and the fastened ply, or hardened washer, or BeS. This equation is based on an even contact across the surface of the bolt head. If a BeS is used under the bolt head, the contact area would move close to the shank resulting in a potential inaccuracy in Equation 7. However, the bolt head is generally the stiffest part of the bolt, meaning that the other parts i.e. shank, threaded part, and threaded portion engaged with the nut, along with the nut itself, are more influential in the bolt's overall stiffness value. Additionally, in presence of BeSs, the solution of the governing equations of the AFC and SFC plies and bolt assemblage behaviour, are generally dominated by the BeS system stiffness, hence this potential inaccuracy in the bolt head stiffness value is insignificant and can be neglected.

$$K_h = \frac{A_{0s}E}{0.3D_{0s}} \tag{7}$$

3.5. Overall bolt longitudinal stiffness:

Considering the bolt head, shank, threaded part between the shank and nut underneath, threaded part engaged with the nut, along with the nut itself as a set of springs in series, as is demonstrated in Figure 7, the bolt longitudinal stiffness is calculated by Equation 8.

$$\frac{1}{K_{bolt}} = \frac{1}{K_h} + \frac{1}{K_s} + \frac{1}{K_t} + \frac{1}{K_{tn}} = \frac{0.3D_{0s}}{A_{0s}E} + \frac{L_{0s}}{A_{0s}E} + \frac{L_{0t}}{A_{0t}E} + \frac{\frac{1+(A_{0n}/A_{0t})}{(A_{0n}/A_{0t})}0.25H_{0n}}{A_{0t}E}$$
$$= \frac{1}{E}\left(\frac{0.3D_{0s} + L_{0s}}{A_{0s}} + \frac{L_{0t} + \frac{1+(A_{0n}/A_{0t})}{(A_{0n}/A_{0t})}0.25H_{0n}}{A_{0t}}\right)$$
$$\xrightarrow{yields} K_{bolt} = \frac{E}{\left(\frac{0.3D_{0s} + L_{0s}}{A_{0s}} + \frac{L_{0t} + \frac{1+(A_{0n}/A_{0t})}{(A_{0n}/A_{0t})}0.25H_{0n}}{A_{0t}}\right)} \tag{8}$$

Defining the total effective length of the bolt shank, L_{es}, and threaded part, L_{et}, as $L_{es} = 0.3D_{0s} + L_{0s}$ and $L_{et} = L_{0t} + \frac{1+(A_{0n}/A_{0t})}{(A_{0n}/A_{0t})}0.25H_{0n}$ respectively, Equation 8 then can be re written as Equation 9.

$$K_{bolt} = \frac{E}{\left(\frac{L_{es}}{A_{0s}} + \frac{L_{et}}{A_{0t}}\right)} \tag{9}$$

4. Joint stiffness:

A bolted joint can be considered as a set of springs loaded in tension and compression. The tightened bolt provides clamping force causing the BeSs and/or plies to be compressed/shortened. Hardened (or round) washer can be regarded as a ply with specific thickness and outside and inside diameters. The bolt preload is in equilibrium with the plies clamping force. The BeSs and/or plies act as a set of springs in series, as is shown in Figure 9. Hence, the plies overall stiffness, K_j, can be calculated by Equation 10.

$$K_j = \frac{1}{\frac{1}{K_1} + \frac{1}{K_2} + \frac{1}{K_3} + \cdots + \frac{1}{K_n}} = \frac{1}{\sum_{i=1}^{n} \frac{1}{K_i}} \tag{10}$$

where n=number of the plies; K_i=i^{th} ply stiffness in the axial direction.

It has been shown using ultrasonic measuring [50] and FEA modelling [51] that the pressure in a bolted joint is greatest under the bolt head/nut and reduces as the distance from the bolt interface increases. The existence of joint surfaces and the joint surfaces finish quality are amongst the factors that have large effects upon the interface pressure distribution and as a result joint stiffness [50].

There are several methods found in the literature to calculate the joint stiffness, such as Cylindrical Stress Field "Q factor", Shigley's Frustum, and finite element method (FEM) based approaches.

4.1. Cylindrical Stress Field "Q factor" approach:

Shigley assumed that the barrel shaped stress field of the plies can be approximated as a cylinder of diameter QD_{0s} [52]. There are several recommendations found in the literature to determine the value of Q. For example, $Q = 3$ was used by Pulling, Brooks et al. [53]. Having the outer and inner diameter of the cylinder i.e. QD_{0s} and $q_i D_{0s}$, it will be possible to determine the i^{th} ply stiffness using Equation 11. The q_i is a coefficient greater than or equal to 1 to consider the clearance between the clamped material and the bolt. Figure 10 shows the cylinder, QD_{0s}, and qD_{0s}.

$$K_i = \frac{A_i E}{t_i} \tag{11}$$

where $A_i = \frac{\pi D_{0s}^2 (Q^2 - q_i^2)}{4}$; t_i=i^{th} ply thickness .

Hence, the plies axial stiffness can be calculated by substituting Equation 11 into Equation 10, as is presented in Equation 12.

$$K_j = \frac{E}{\sum_{i=1}^{n} \frac{t_i}{A_i}} = \frac{\pi E D_{0s}^2}{4 \sum_{i=1}^{n} \frac{t_i}{(Q^2 - q_i^2)}} \tag{12}$$

There are other attempts found in the literature aiming to increase the accuracy of the Q factor approach [52], albeit by making the approach more complex. It is worth noting that the AFC cleat and SFC middle plate have slotted holes which make the whole connection plies slightly less stiff than the case if the plies all had normal holes. This difference in the plies stiffness is assumed to be negligible. Additionally, using BeSs can change the load distribution pattern in the plies. However, the overall stiffness of the joint with BeSs is dominated by the BeSs stiffness. Hence, any inaccuracy in calculating the joint plies stiffness when BeSs are used is insignificant, and is therefore considered as for the case without BeSs.

4.2. Shigley's frustum approach:

Shigley, Budynas et al. [54] used an approach considering that the bolted plies stress field shape looks like a frustum of a hollow cone. To apply this approach, a dispersion angle is assumed for the stress distribution in the plies i.e. α (see Figure 11). By taking integration over the ply thickness based on an arbitrary clamping force, F, each ply deflection and as a result stiffness can be calculated. Considering a ply element of the thickness dx, as shown in Figure 11, the ply element deflection, dL_p, due to the clamping force, F, is calculated by Equation 13.

$$dL_p = \frac{F dx}{E A_e} \tag{13}$$

where A_e is the element area calculated by Equation 14.

$$A_e = \pi \left[\left(x \tan \alpha + \frac{D}{2} \right)^2 - \left(\frac{d}{2} \right)^2 \right] = \pi \left(x \tan \alpha + \frac{D + d}{2} \right) \left(x \tan \alpha + \frac{D - d}{2} \right) \tag{14}$$

where D and d are shown in Figure 11. By substituting Equation 14 into Equation 13, and taking integration over the ply depth, the ply deflection, ΔL_p, under the clamping force, F, is calculated by Equation 15.

$$\Delta L_p = \frac{F}{\pi E}\int_0^{t_i} \frac{dx}{\pi\left(x\tan\alpha + \frac{D+d}{2}\right)\left(x\tan\alpha + \frac{D-d}{2}\right)}$$

$$= \frac{F}{\pi E d \tan\alpha}\ln\frac{(2t_i\tan\alpha + D - d)(D+d)}{(2t_i\tan\alpha + D + d)(D-d)} \tag{15}$$

The i^{th} ply stiffness is calculated by Equation 16.

$$K_i = \frac{F}{\Delta L_p} = \frac{\pi E d \tan\alpha}{\ln\left(\frac{(2t_i\tan\alpha + D - d)(D+d)}{(2t_i\tan\alpha + D + d)(D-d)}\right)} \tag{16}$$

A dispersion angle $\alpha = 45°$ has been used [54] and is also suggested for the stiff bearing length by NZS3404 [28]. However, it has been reported that this angle overestimates the joint clamping stiffness, a range of $15° \leq \alpha \leq 33°$ is recommended for the most cases and $\alpha = 30°$ is recommended in general [54]. D is the outside diameter of the bolt head, or nut, or hardened washer, or BeS, or is calculated for the neighbouring ply stress distribution. Using BeSs can change the stress distribution pattern, especially in the underneath ply onto which the BeS is bearing, however the overall joint stiffness value is dominated by the BeS stiffness and this change of the ply stress distribution, that has an influence on the AFC and SFC plies stiffness, is negligible.

To apply the frustum approach, the mid-plane of the joint is located to construct two equilateral triangles, one above and one below the mid-plane of the joint. Each one of these regions' dimensions are used to define the individual frustra stiffness, and subsequently the whole joint plies stiffness. The joint overall stiffness, K_j, then is calculated by Equation 10.

For the AFC cleat and SFC middle plate, the integration of the Equation 15 can be calculated considering having the slotted hole instead of normal circular hole, which will result in slightly lower joint plies stiffness. However, this difference is negligible.

4.3. Other approaches:

Wileman, Choudhury et al. [51] used finite element analysis to determine the stiffness of two plies made of the same material. Their method was then extended by other researchers to be applicable to two materials and address more effects such as variable bolt head diameters [55, 56].

The other possibility to calculate plies stiffness is conducting the experimental tests to determine the load-deflection curve of the plies under the compression in the laboratory by simulating the practical conditions. The Fastener Engineering and Design Support manual [57] states that a bolt is often about 1/3-1/5 as stiff as the joint that it is being used in. This is a rough estimation and it is recommended instead to calculate the AFC and SFC plies stiffness for research/design purposes using one of the methods explained above.

5. Belleville spring(s) stiffness

Belleville springs (BeSs), known also as “disc springs, Belleville washers, and conical compression washers” are truncated conical annual washer-type elements invented by Julien Belleville in 1867 [58]. A heavy-duty BeS is usually made of high strength steel. A BeS is characterised by four main geometrical variables including outside and inside diameters, thickness, and maximum deflection. Figure 12 shows the typical cross sectional layout of a BeS. A BeS compresses to a flat disk under a defined level of force known as the flat load. A well accepted analytical approach to correlate the BeS flat load to the material and geometrical characteristics was proposed by Almen and Laszlo [59]. A common application of BeSs is anywhere that a bolt pre-load is needed to be maintained over the time, hence they come in a wide range of rated strength and sizes and are usually similar in size to standard washers, so can be used in conventional layout bolted connections. When subjected to a bolt tension loss, for example, as a result of stress relaxation, the BeS pushes out to compensate for part of the bolt tension loss. This action is mathematically formulated in this paper.

A BeS will be elastic up to full squash load and release, provided that it is supplied pre-set. Pre-setting involves preloading the springs to the flat position prior to their use, which is part of the manufacturing process for most of the BeSs [60]. Not all BeSs are pre-set, however it is recommended that any used for the AFC and SFC are pre-set so that they operate elastically in service.

The ideal load-deflection curve of a BeS is linear [61]. Typically the BeSs have a bilinear load-deflection curve which is linear up to 80-90% (for higher load BeSs to be used, for example, in bolted joints) or >95% (for thinner BeSs to be used, for example, in machine elements) of the flat load, and after that point the load increases progressively as the spring begins to bottom out (roll on) [62, 63] (Figure 13). This is because the lever arm of the bending force acting on the BeSs' edge from the underneath plate suddenly decreases slightly and requires higher additional imposing force to further flatten the BeS, when it reaches >80% of the flat load.

The loading and unloading curves of the BeSs are not exactly the same i.e. there is a hysteresis curve which is resulting from the friction between the spring edge and the underneath plate surface causing an amount of energy to be dissipated (Figure 13). A smoother and rounder BeS edge may cause less energy dissipation on a given underneath surface.

Assuming a linear behaviour for a BeS, two different values for BeS stiffness associated with the loading and unloading can be defined i.e. $K_{BeS,loading}$ and $K_{BeS,unloading}$. $K_{BeS,loading}$ may be considered in the calculations associated with the installing and tightening the bolts as well as when an un-flattened BeS is being squashed further in service due to, for example, prying and/or AFC bolt additional axial force in double curvature state. $K_{BeS,unloading}$ may be considered in the calculations associated with the operation of the BeS in service when it pushes out due to the bolt tension loss. However, these two stiffness values for a single BeS with well-rounded and smooth edge are often very close and the small difference is mainly in an offset value due to the loss of energy. Hence, it is recommended to define a unique value for a BeS stiffness i.e. K_{BeS}. If the BeS edge is not well-rounded and smooth, and/or if two or more BeSs are used in parallel configuration, which is explained below, the amount of the energy loss would be higher resulting in more different behaviour in loading and unloading paths. In such case, which is recommended to be avoided in practice, the loading and unloading paths should be regarded separately for design purposes.

Part of the dissipated energy during squashing a BeS is the localized plastic deformations of the underneath plate (roughness) due to the contact pressure along the edge of the BeSs and the outer plies. A potential solution to minimize this effect may be using flat hardened washers with large outside diameter between the BeSs and the connection’s outer ply.

To determine the BeS stiffness, one can fit the best straight line to the load-deflection data points of BeS loading and unloading paths that are often provided by the BeS manufacturer for each product. The slope of these loading and unloading lines are often very close and can either be a good estimation of the BeS stiffness, K_{BeS}. The other possibilities are taking an average of the slopes of the loading and unloading lines or to fit a line on both loading and unloading paths at the same time to represent the BeS stiffness. The latter is recommended. A preliminary estimation of the BeS stiffness may be calculated by dividing the BeS flat load by its maximum deflection. This may not be necessarily always accurate specifically if the BeS load-deflection curve is bi-linear.

BeSs can be assembled in various ways including series, parallel, and series/parallel, as shown in Figure 14. If n similar BeSs are used in parallel, the flat load of the system will be n times the flat load of a BeS, and the maximum deflection of the BeSs system remains the same as for a single BeS's, resulting in a stiffer system than one BeS. The reason is that the force required to bend the edge of the paralleled BeSs will be n times the force required to bend a single BeS edge, if the shear stress transfer between the BeSs surfaces is ignored. Thus, the stiffness of such system, $K_{BeS,P}$, can be calculated by Equation 17. It is recommended not to use more than 4 springs in parallel unless considering an appropriate higher safety factor to compensate for loss of energy due to friction between the springs [64]. Additionally, if a single BeS can be used, as opposed to multiple BeSs in parallel, the total material needed to achieve the target load and deflection is less than multiple BeSs in parallel, hence is more cost effective to use the single BeS.

$$K_{BeS,P} = \underbrace{K_{BeS} + K_{BeS} + \cdots + K_{BeS}}_{n} = n \times K_{BeS} \tag{17}$$

If n similar BeSs are used in series, the flat load of the system remains the same as a BeS's, and the maximum deflection of the system will be n times the maximum deflection of a BeS, resulting in a softer system than one BeS. Thus, the stiffness of such system, $K_{BeS,S}$, can be calculated by Equation 18. To prevent in-service instability and lateral movement, it is recommended to keep the number of BeSs in series as small as possible [65].

$$K_{BeS,S} = \frac{1}{\underbrace{\frac{1}{K_{BeS}} + \frac{1}{K_{BeS}} + \cdots + \frac{1}{K_{BeS}}}_{n}} = \frac{1}{\frac{n}{K_{BeS}}} = \frac{K_{BeS}}{n} \tag{18}$$

Figure 15 shows the ideal linear load-deflection graphs of a single BeS as well as two and three similar BeSs in series and parallel. If a BeS load-deflection curve is bilinear due to rolling on, one can define two stiffness values for the BeS equal to slope values of the two lines of either loading or unloading graphs, as is shown in Figure 13.

If m groups of stacked-in-parallel BeSs are stacked in series, where n_i is the number of BeSs in the i^{th} group, the overall stiffness of the BeSs system, $K_{overall,SP}$, until reaching the flat load of the weakest group(s), can be calculated by Equation 19, as from that point onwards, the weak group(s) is flat and should be ignored for the BeS system stiffness calculations.

$$K_{overall,SP} = \frac{1}{\frac{1}{n_1 K_{BeS}} + \frac{1}{n_2 K_{BeS}} + \cdots + \frac{1}{n_m K_{BeS}}} = \frac{1}{\sum_{i=1}^{m} \frac{1}{n_i K_{BeS}}} = \frac{K_{BeS}}{\sum_{i=1}^{m} \frac{1}{n_i}} \tag{19}$$

The overall stiffness of two different BeSs in parallel, if they can be practically stacked in parallel, is the summation of two BeSs stiffness values. However there are practical considerations in using two different BeSs in parallel.

The overall stiffness of two different BeSs, namely BeS_1 and BeS_2, in series, is $K_{overall,s} = \frac{K_{BeS1} \times K_{BeS2}}{K_{BeS1} + K_{BeS2}}$ until reaching the weaker BeS flat load, as from that point onwards, the weaker BeS is flat and the BeSs system stiffness is equal to the stronger BeS stiffness. An example of such application may be using one type of BeS at bolt head side and the other type at the nut side of a bolted connection. It is recommended to use only one type of BeS in practice to minimize the probable construction errors.

6. AFC or SFC bolt installation and post-sliding tension loss with and without BeSs:

This section presents two examples of the AFC or SFC plies and bolt assemblage with and without BeSs, calculates a nut rotation required to tighten the bolts in the elastic range at installation, and demonstrates the BeSs ability in retaining the post-sliding bolt tension (or clamping force) of the connection, when the bolt undergoes post sliding plastic elongation and/or the plies undergo post sliding reduction in their thickness and come back to the initial position following a few cycles of sliding. To this end, the stiffness values of the connection's components per bolt are first calculated. These components are the joint plies, hardened washer(s) or BeS(s), and bolt. To calculate the bolt stiffness value, the only unknown value would be the initial length of the bolt contributing threaded portion between the shank and nut underneath, L_{0t}, to clamp the joint by a given preload. This has a unique value for a given bolt tension and is calculated using Equations 1, 2, 6, and 7 as well as considering the displacement compatibility (the bolt deformation once the bolt is tightened must be compatible with the joint plies' and hardened washer(s)' or BeS' deformations). At this stage the nut rotation to tighten the bolt is calculated considering the displacement compatibility and the bolt thread's pitch. Then the stiffness values of the connection's components are re-calculated, this time, considering the bolt longitudinal plastic deformation, δ_b, and joint plies thickness reduction, δ_p, which are both variable. Finally, considering the connections' post-sliding displacement compatibility as well as force equilibrium per bolt, the post sliding bolt tension, which is a function of two variables (δ_b and δ_p), is derived. These calculations are performed for each case with and without BeSs and are shown in Table 2. This table also presents the sources for each step of calculations. Figure 16 schematically shows the proposed spring models of both cases.

6.1. AFC or SFC without BeSs:

An AFC or SFC with a cap plate (or outer plate), shim, cleat (or middle plate), shim, and beam bottom flange (or other outer plate) of 16, 5, 16, 5, and 16mm thickness respectively is considered. The plies are intended to be clamped by 100mm long "excluding the bolt head height" High Strength Friction Grip (HSFG) property class 8.8 (G8.8) M20 bolt. The bolt is intended to be tightened up to 145kN, which is approximately equivalent to the minimum HSFG G8.8 M20 bolt proof load given in AS/NZS 1252 [66]. This is the peak point of the bolt elastic behaviour range. The initial bolt shank length is 50.2mm as the average of the minimum and maximum values identified by AS/NZS 1252 [66]. According to NZS 3404 [28], $A_{0t} = 245mm^2$ and the bolt pitch is 2.5mm. The average values of the maximum and minimum of two different outside nut diameters are shown in Figure 17, in accordance with AS/NZS 1252 [66]. As an average of the maximum and minimum values identified by AS/NZS 1252 [66], $H_{0n} = 20mm$.

The steel elastic modulus is considered as $E = 205\ GPa$ as specified by NZS 3404 [28], and the coefficients Q and q_i are considered 3 and 1.1 respectively. The latter is to satisfy 2mm hole size clearance recommended in NZS 3404 [28]. Two 3.85mm thick hardened washers with outside and inside diameters of 41.2mm and 22.3mm respectively, are used at the bolt head and nut sides (Figure 17). These values are the average of the maximum and minimum values identified by AS/NZS 1252:1996 [66] for the hardened (or round) washers for high strength structural bolting. The following values then can be calculated according to Table 2 for joint's pre and post sliding stages:

Step a1)

$$K_{plies} = \frac{\pi \times 20^2(3^2 - 1.1^2) \times 205}{4 \times (16 + 5 + 16 + 5 + 16)} = 8650kN/mm \quad (20)$$

Step a2)

$$K_{hardened\ washer} = \frac{hardened\ washer\ area \times E_{steel}}{hardened\ washer\ thickness}$$

$$= \frac{\pi(41.2^2 - 22.3^2) \times 205}{4 \times 3.85} = 50265kN/mm \tag{21}$$

Step b1)

$$K_j = \frac{8650 \times (50265/2)}{(50265/2) + 8650} = 6435kN/mm \tag{22}$$

Step c)

$$\Delta L_j = \frac{145}{6435} = 0.02mm \tag{23}$$

Step d)

$$\frac{A_{0n}}{A_{0t}} = \frac{\left(\frac{\pi}{4} \times \left(\frac{38.3 + 33.5}{2}\right)^2\right) - 245}{245} = 3.13 \tag{24}$$

Step e)

$$\underbrace{\left[\left(\frac{145}{\frac{314 \times 205}{50.2}}\right) + 50.2\right]}_{elongated\ shank\ length} + \underbrace{\left[\left(\frac{145}{\frac{245 \times 205}{L_{0t}}}\right) + L_{0t}\right]}_{length\ of\ elongated\ threaded\ part\ between\ the\ shank\ and\ nut\ underneath}$$

$$+ \underbrace{\frac{145}{\frac{314 \times 205}{0.3 \times 20}}}_{head\ deformation} + \underbrace{\frac{145}{\frac{3.13 \times 245 \times 205}{(1 + 3.13) \times 0.25 \times 20}}}_{deformation\ of\ the\ engaged\ bolt\ threaded\ part\ along\ with\ the\ nut}$$

$$= \underbrace{58 + (3.85 \times 2) - 0.02 = 65.7}_{compressed\ joint\ grip\ length} \xrightarrow{yields} L_{0t} = 15.2mm \tag{25}$$

Step f)

$$\propto_{Nut} = \frac{58 + (3.85 \times 2) - 50.2 - 15.2}{2.5} \times 360 = 30.2\ degrees \tag{26}$$

Step g)

$$K_{bolt} = \frac{205}{\left(\frac{(0.3 \times 20) + 50.2}{314} + \frac{15.2 + (\frac{1 + 3.13}{3.13} \times 0.25 \times 20)}{245}\right)} = 764kN/mm \tag{27}$$

Step h)

$$K_{plies-ps} = \frac{\pi \times 20^2(3^2 - 1.1^2) \times 205}{4 \times (58 - \delta_p)} = \frac{501697}{(58 - \delta_p)} kN/mm \tag{28}$$

Step i)

$$K_{j-ps} = \frac{\frac{501697}{(58 - \delta_p)} \times (50265/2)}{(50265/2) + \frac{501697}{(58 - \delta_p)}}$$

$$= \frac{2.52 \times 10^{10}}{(1003393) + (50265 \times (58 - \delta_p))} kN/mm \tag{29}$$

Step j)
$$\begin{cases} \dfrac{2.52 \times 10^{10}}{(1003393) + \left(50265 \times \left(58 - \delta_p\right)\right)} \times \overbrace{\Delta L_{joint}}^{\text{joint compression}} = 764 \times \overbrace{\Delta L_{bolt}}^{\text{bolt deformation}} \\ \Delta L_{joint} + \Delta L_{bolt} = \left(\underbrace{65.7}_{58+(3.85\times 2)} - \delta_p \right) - \left(\underbrace{65.5}_{50.2+15.2} + \delta_b \right) = 0.21 - (\delta_b + \delta_p) \end{cases} \tag{30}$$

Step k)
$$T_{bolt-ps} =$$
$$\begin{cases} \dfrac{1.93 \times 10^{13} \times (0.21 - (\delta_b + \delta_p))}{\left\{\left[(1003393) + \left(50265 \times \left(58 - \delta_p\right)\right)\right] \times 764\right\} + (2.52 \times 10^{10})}; (\delta_b + \delta_p) < 0.21mm \\ 0;\ (\delta_b + \delta_p) \geq 0.21mm \end{cases} \tag{31}$$

6.2. AFC or SFC with BeSs:

The AFC or SFC of the section 6.1 example is intended to be clamped by the same bolt but with two BeSs in series, one at head and the other at nut side of the bolt, instead of the two hardened washers. Each BeS is as thick as a hardened washer, i.e. 3.85mm. The BeS flat load is 145kN with the maximum deflection of 1mm. The BeSs are assumed to be just flattened after bolt tightening, hence there is no post tightening compression considered along BeSs' thickness. The load deflection graph of this BeS is linear, hence each BeS stiffness is $K_{BeS} = 145kN/mm$. Results of the steps d), e), g) and h) are the same as the values calculated in section 6.1. The following values then can be calculated for this joint's pre and post sliding stages:

Step a2)
$$K_{BeS} = 145kN/mm \tag{32}$$

Step b2)
$$K_{j-BeS} = \frac{8650 \times 145}{145 + (2 \times 8650)} = 71.9kN/mm \tag{33}$$

Step c)
$$\Delta l_{plies} = \frac{145}{8650} = 0.02mm \tag{34}$$

Step f)
$$\propto_{nut-BeS} = \frac{58 + ((3.85 + 1) \times 2) - 65.5}{2.5} \times 360 = 318\ degrees \tag{35}$$

Step i)
$$K_{j-ps-BeS} = \frac{\dfrac{(501697/2)}{(58 - \delta_p)} \times 145}{(145/2) + \dfrac{501697}{(58 - \delta_p)}} = \frac{72.7 \times 10^6}{(1003393) + (145 \times \left(58 - \delta_p\right))} kN/mm \tag{36}$$

Step j)

$$\begin{cases} \dfrac{72.7 \times 10^6}{(1003393) + (145 \times (58 - \delta_p))} \times \Delta L_{joint} = 764 \times \Delta L_{bolt} \\ \Delta L_{joint} + \Delta L_{bolt} = \left(\underbrace{67.7}_{65.7+2} - \delta_p\right) - (65.5 + \delta_b) = 2.21 - (\delta_b + \delta_p) \end{cases} \quad (37)$$

Step k) $T_{bolt-ps-BeS} =$

$$\begin{cases} \dfrac{5.56 \times 10^{10}\left(2.21 - (\delta_b + \delta_p)\right)}{(72.7 \times 10^6) + \left[\{(1003393) + (145 \times (58 - \delta_p))\} \times 764\right]} ; (\delta_b + \delta_p) < 2.21mm \\ 0;\ (\delta_b + \delta_p) \geq 2.21mm \end{cases} \quad (38)\ (37)$$

Figures 18 and 19 show the post-sliding bolt tension for cases with and without BeSs, $T_{bolt-ps}$ and $T_{bolt-ps-BeS}$, versus the variable bolt perfectly plastic longitudinal deformation and/or variable plies thickness reduction. Figure 18 shows that the BeSs could maintain the post-sliding bolt tension equal to 90% of the bolt installed tension, at the point at which the same bolt tension loss factors cause the bolt to lose all of its preload without BeSs. Ramhormozian, Clifton et al. [38] experimentally showed that the average post sliding bolt tension loss for the AFC test samples using ¾ inch imperial black bolts of property class 10.9 was about 62% for the cases with the installed bolt tension of 50% to 60% of the bolt proof load, while using two customized BeSs at head and nut sides of the AFC bolts could retain an average of about 80% of the installed bolt tension, suggesting the significant benefit of the BeSs in retaining the bolt tension.

7. Using not flattened Belleville springs to minimize the prying effects and to improve the AFC self-centring capability:

The SHJ relative beam to column rotation can potentially apply additional tension to the beam bottom flange level AFC bolts, because of the prying effects. These effects occur because the bottom flange cleat is welded at one end to the column and therefore describes an arc as the column rotates, while the other end of the cleat is bolted to the beam underside, which effectively remains horizontal. This will result in an external potential overstretching force imposed on the bolted friction connection. Prying effects can also occur in other applications of the AFC and SFC, for example, in braces, column bases, and rocking shear walls. Prying actions can change the faying forces on the sliding interfaces and increase the tensile load on the bolts. To demonstrate the concept of prying effects on the AFC or SFC, the following approach is presented including showing the benefit of using not flattened BeSs to minimize this undesirable effect.

Consider two SHJ beam bottom flange level AFCs same as the section 6 examples' joints, this time, with the bolt installed tension equal to 80% of the bolt proof load i.e. $0.8 \times 145 = 116kN$. L_{0t} and K_{bolt} for the cases without and with BeSs are calculated as 15.33mm and 763kN/mm, and 15.73mm and 759kN/mm respectively. The post-tightening deformation of the cap plate (or beam bottom flange), shim, and cleat are calculated as $\Delta l_{CSC} = \frac{116}{\frac{\pi \times 20^2(3^2-1.1^2)\times 205}{4\times(16+5+16)}} = 0.01mm$. The prying induced joint expanding actions on these AFCs can be simulated as the applied forces F_{prying} on the interface of the cleat and the lower shim, and the outer face of the beam bottom flange, as is shown in Figure 20. The displacement associated with F_{prying} is denoted by δ_{prying}. Increasing F_{prying} initially causes δ_{prying} to increase from zero to Δl_{CSC}. At this point, the faying force on the interface of the cleat and the upper shim (upper faying force) is reduced to zero while the bolt tension and the faying force on the interface of the cleat and the lower shim (lower faying force) are slightly increased to 122kN and 117kN for the cases without BeSs or with flattened BeSs and with not flattened BeSs respectively. From this point, by increasing δ_{prying}, the bolt tension and the lower faying force increase elastically up to the bolt proof load while the upper faying force remains zero. The total faying force at each stage, which is directly related to the joint sliding resistance, is the summation of upper and lower faying forces.

To calculate the variations of the bolt tension and faying forces due to the varying prying actions, it is necessary to calculate the stiffness of the parts of the AFC which contribute in carrying the prying loads. These are bolt, cap plate, lower shim, and hardened washers (or BeSs) for the cases without (or with) BeSs, all acting as a set of springs in series. These stiffness values are denoted by K_{jp} and K_{jp-BeS} and are calculated as 718kN/mm and 66kN/mm respectively. Figure 21 shows the variations of the joint forces per bolt including the bolt tension, lower faying force, upper faying force, and total faying force under the prying actions for the cases without BeSs or with flattened BeSs and with not flattened BeSs. Note that if two BeSs as thick as the hardened washers but with the flat load of less than the installed bolt tension (i.e. 116kN) are used in this joint, instead of the hardened washers, the joint behaviour under prying actions is identical to that of with hardened washers.

The threshold of δ_{prying} to ensure that the bolt is not plasticized is 0.04mm and 0.44mm for the cases without BeSs or with flattened BeSs and with not flattened BeSs respectively, as is shown in Figure 21. In other words, in this example, the axial displacement capacity of the joint with not flattened BeSs to accommodate the elastic prying expansion is 11 times of that of the joint with flattened BeSs or without BeSs, and the variations of the joint forces are significantly less sensitive to the prying actions with not flattened BeSs. This means that the joint with not flattened BeSs can limit the prying bolt tension increase to 2.3% of the installed bolt tension (i.e. 119kN), at the point at which the same bolt reaches the proof load (i.e. 145kN), by 25% prying bolt tension increase with respect to the installed bolt tension, in the joint without BeSs or with initially flattened BeSs. Thus the use of not completely flattened BeSs is recommended to reduce the negative effects of the prying on the AFC and SFC sliding behaviour where they are susceptible to these effects.

Moreover, the presence of the not fully compressed BeSs under both bolt head and nut generate an elastic rotational spring which allows the bolt to develop the asymmetric friction sliding in part by rotating as a partially rigid body with elastic end springs. This generates a couple in the system per bolt, which are horizontal components of the bolt tension in stable sliding state, acting in the opposite direction of the sliding direction, hence enhancing the self-centring capability of the AFC and potentially the overall structural system and building. Figure 22 shows the self-centering components due to the bolt-body rotation attributed to the use of not flattened BeSs. This effect has been observed at real scale component level in the experiments of non-prying AFC test setup [67] and SHJ beam bottom flange AFC test setup [37] undertaken by Ramhormozian, Clifton et al.

8. Other potential benefits of using Belleville springs in the AFC and/or SFC:

Belleville springs can distribute the bolt tension resulted clamping force on the join plies over a wider area compared with hardened washers particularly when they are used under the bolt head and nut, hence are expected to decrease the post sliding wearing of the sliding surfaces, conventionally localized around the holes. This effect was observed in the AFC experiments without and with customized BeSs undertaken by Ramhormozian, Clifton et al. [38]. This may also increase the whole joint frictional resistance for a given clamping force, resulting from potential wider contact area on the sliding surfaces as is observed in the experiments undertaken by Ramhormozian, Clifton et al. [32].

The moment and shear interaction in the AFC bolts tries to rotate the bolt head and nut while the bolt is in double curvature state. The not flattened BeSs under the nut and bolt head provide more rotational flexibility to allow the bolt head and nut to rotate with expected potential smaller internal actions generated in the bolt.

Using BeSs can significantly decrease the AFC and SFC bolt tension change due to the nut rotation as is shown in the examples of sections 6.1 and 6.2. This makes it potentially possible to reach a precise level of the elastic bolt tension using an appropriate turn-of-nut based method. This is being researched by the authors. Use of the BeSs can also decrease the bolt tension drop of the formerly-tightened bolts of each joint during installation. This effect was observed in a set of non-prying AFC sliding experiments undertaken by Ramhormozian, Clifton et al. [38] using customized BeSs.

Using not flattened BeSs can decrease the bolt tension change during sliding. These can be loss of the bolt tension due to the reasons which are discussed in this paper, or transient increase in the bolt tension during sliding when the sliding surface particles are removed from the surfaces and potentially increase the bolt grip length, and/or when two surface waviness peaks face each other, and/or when the increase in temperature expands the plies hence increases the bolt grip length. This provides the whole joint with more stable behaviour as is observed experimentally [37]. Ramhormozian, Clifton et al. [32, 38] experimentally measured the post sliding temperature change of the AFC bolts and cleat for two sets of experiments on the SHJ beam bottom flange and non-prying AFC test setups using HSFG PC8.8 M20 and ¾ inch imperial black bolts of property class 10.9 respectively, all installed within the bolts elastic range, with reported insignificant temperature rise of not more than 4 degrees Centigrade. However, the temperature gradient during sliding may be potentially significant specifically for the large bolt sizes with very high clamping force.

Using BeSs can potentially decrease the in service AFC and SFC bolt tension loss due to the factors such as relaxation, creep, and vibration induced self-loosening based on the concepts discussed in the current paper. Vibration induced self-loosening is the nut-bolt relative rotation which is well known to be more susceptible to occur for the lower bolt tensions. Hence, by retaining the bolt tension through the use of BeSs, the chance of the self-loosening is also decreased. Moreover, the amount of the bolt tension drop due to a given potential bolt-nut relative rotation during vibration is much lower for the case with BeSs than that of the case without BeSs, as the bolt/BeS assemblage longitudinal stiffness is much smaller than that of bolt/hardened washer assemblage.

9. Proposed design procedure for using BeSs in the AFC and SFC:

The following steps are recommended to be followed to use BeSs in the AFC and/or SFC. It is recommended to use only two BeSs in series, one under the bolt head and one under the nut, for any application of the AFC and SFC.

I. Determining the required installed bolt tension T_i. This is strongly recommended to be within the bolt elastic range, and not in post-yield range, to decrease the initial post-tightening bolt tension loss and joint creep [44], and to avoid yielding the bolt material during joint sliding. This is critical for the AFC and SFC with slotted outer plates layout as the bolt is under additional tension, shear, and bending moment during stable sliding state. Additionally, installing these bolts well in the elastic range will cause the bolts to deform elastically, which is recoverable upon load removal, hence is expected to improve the self-centering ability of the system. The lower clamping force on the AFC and SFC plies may also potentially reduce the localized bearing stress and as a result post sliding thickness reduction of the AFC and SFC plies. Note that the elastically tensioned bolt delivers smaller clamping force compared with the conventional part-turn based fully tensioned bolt, especially in the pre-sliding state of the connection. This needs to be carefully taken into account in the design of the connection, and if is required, larger number of bolts and/or bigger size bolts and/or higher grade bolts may be used in case of considering elastic installed bolt tension instead of the conventional part-turn induced bolt tension. As it is already mentioned, the use of BeSs may also potentially increase the frictional resistance of the connection for a given clamping force, compensating for the lower installed bolt tension. On the other hand, very low levels of the installed bolt tension may increase the susceptibility of the bolt to vibration induced self-loosening, hence is recommended to be avoided. It is also recommended to consider a safety factor for the installed bolt tension to compensate for the initial bolt tension loss (within the first ten seconds after the bolt is tightened), short term loss (within the first twelve hours after the bolt is tightened) and long term loss (asymptotical over the joint design life after the bolt is tightened), and effect of tightening a group of bolts. The initial, short term, and 20-year long term bolt tension loss, as the percentage of the initial bolt tension, is observed and extrapolated as 2.9, 9.6, and 16.8 respectively for the bolts in absence of BeSs [68]. Additionally, while tightening a group of bolts, tightening the latter bolts may result in bolt tension loss of the former bolts. The use of BeSs may significantly decrease these initial, short term, long term, and group tightening bolt tension losses, as can be justified by the same concept as that is shown in Figure 19, requiring much smaller safety factor.

II. Determining the geometrical limitations of the BeSs to be used. These may include maximum possible OD to distribute the clamping force as widely as possible, ID to provide appropriate guide (i.e. bolt) for the BeSs and to satisfy hole size clearance requirement, and overall height. Note that there is no need to use any hardened washer under the rotating part of the bolt (i.e. nut in most applications) in presence of the BeS, provided the BeS hardness value is greater than or equal to that of the conventional hardened washer. If is required, the BeS operating temperature and surface finish can also be determined. The latter is recommended to match the bolt finish, either natural finish, or black oxide, or zinc phosphate.

III. Calculating the flat load of the BeSs. For any application of the AFC and for the SFC which is prone to prying effects, this is recommended to be βT_i, and for the SFC which is not prone to prying effects to be γT_i where $Max\ of\ \left\{\frac{Bolt\ proof\ load}{T_i}\right\}\ and \left\{\frac{1}{\underbrace{0.8}_{to\ partially\ squash\ the\ BeS}} \times \frac{1}{\underbrace{0.8\sim0.9}_{to\ \ neglect\ the\ BeS\ post\ rolling\ on\ state\ flexibility}}\right\} \leq \beta$, and $Max\ of\ \left\{\frac{Bolt\ proof\ load}{T_i}\right\}\ and\ \left\{\frac{1}{0.8\sim0.9}\right\} \leq \gamma$. This is to ensure that the BeS is always not fully flattened before the bolt tension reaches to its proof load. However, this condition may be relaxed to fit the practical constraints if there was any.

IV. Determining the maximum linear deflection of the BeSs. This is the maximum BeS deflection until it starts to roll on. For any application of the AFC and for the SFC which is prone to prying effects, this is recommended to be at least $(0.8\sim0.9)\beta$ in mm, and for the SFC which is not prone to prying effects to be at least $(0.8\sim0.9)\gamma$ in mm. This ensures that, for any application of the AFC and for the SFC which is prone to prying effects, each BeS deflects at least by 1mm from zero load until reaching the installed bolt tension, and still having at least 0.25mm of capacity to deflect until reaching 80% to 90% of its flat load, and for the SFC which is not prone to prying effects, each BeS deforms at least 1mm at installation until reaching 80% to 90% of its flat load.

V. Satisfying all the requirements of parts II, III, and IV, the optimum BeS, with the aim of providing the maximum ability to compensate for any potential bolt tension loss, is the one with the highest ratio of $\frac{Maximum\ BeS\ linear\ deflection}{BeS\ flat\ load}$. This ensures that the BeS to be used, delivers the maximum possible deformation until reaching the installed bolt tension. The optimum BeS can be either chosen from the supplier's available stock or requested to be customized. If there is any specific application of the BeS, for example, requiring larger post tightening capacity until reaching 80% to 90% of its flat load, the BeS needs to be designed to fit the specific purpose.

Example: The intension is to design the BeSs for a SHJ beam bottom flange level AFC HSFG property class 8.8 M20 zinc phosphate coated bolts. The design bolt tension is considered as 90kN. The minimum horizontal distance between the plies holes' centres and from the plies' holes centres to the plies' edge are 80mm and 35mm respectively. The normal holes diameter is 22mm. The heavy duty BeS load-deflection curve is assumed to be linear up to 85% of its flat load.

Solution: I) T_i=90kN, II) OD<minimum of {2×35 and 80}=70mm, ID=22mm to be compatible with the normal holes' size, and overall height<10mm to allow enough construction clearance, and the surface finish is recommended to be zinc phosphate, III) Max of {145/90}and{1/(0.8×0.85)}=1.6≤β, hence 1.6×90=144kN≤BeS flat load, IV) 0.85×1.6=1.4mm≤Maximum linear deflection of BeS, V) Satisfying all the requirements of parts II, III, and IV, the optimum BeS, to be chosen from the available stock or customized, is the one with the highest ratio of $\frac{Maximum\ BeS\ linear\ deflection}{BeS\ flat\ load}$.

10. Conclusions:

1) AFC and SFC are two types of SBCs. The AFC is an energy dissipating component used in the SHJ and other types of seismic resisting systems. It develops a non-linear inelastic force-displacement curve during sliding. The AFC bolts are under MVP interaction during stable sliding causing the conventionally fully tensioned AFC bolts to plastically deform and lose part of their preload. This can also be the case for the SFC with slotted outer plated layout. The AFC and SFC bolts may be under the prying actions that may potentially plastify the bolts and result in bolt tension loss. Moreover, in addition to potential initial, short term, and long term bolt tension loss, the high clamping force generated by the bolts causes the post-sliding wearing and thickness reduction of both AFC and SFC plies resulting in the further bolt tension drop.
2) All AFC and SFC components i.e. plies, bolt assemblages, and BeSs act as the springs with different values of the stiffness. The formulations of calculating the stiffness value for each one of the AFC and SFC components are proposed in this paper.
3) Installing the bolts in their elastic range decreases the probability of the bolt tension loss by increasing the bolt capacity to accommodate the elastic deformations, and potentially decreases the AFC and SFC plies post-sliding thickness reduction probability. This may also improve the AFC self-centring capability. However, the elastically preloaded bolts deliver smaller pre-sliding clamping force compared with the fully tensioned bolts based on the part-turn method of tightening. This effect needs to be taken into account to design the connection. It is shown analytically in this paper that BeSs can considerably

reduce the post-sliding AFC and SFC bolt tension loss. Using BeSs considerably reduces the AFC and SFC bolts sensitivity to the group tightening losses after installation, and to the seismic bolt tension loss factors, in which the latter are more critical. Hence, the post-sliding bolt tension variability of different bolts of the AFC and SFC incorporating the BeSs would be less than the AFC and SFC with no BeS. This provides the AFC and SFC with more consistent and predictable seismic behaviour.

4) Installing the BeSs in not flattened state provides a degree of both axial and rotational flexibilities under the bolts head and/or nut causing to improve the AFC self-centering capability, and to reduce the possibility of the AFC and SFC bolt to be plastically stretched due to the prying actions. This is in comparison with the case with no BeSs or with flattened BeSs.
5) Using BeSs can be potentially beneficial in reducing the post sliding AFC and SFC plies wearing, reducing the AFC bolts stable sliding additional internal actions, minimizing the AFC and SFC bolt tension variations during bolt tightening and sliding, and reducing the in service AFC and SFC bolt tension loss.
6) A design procedure for using BeSs in the AFC and SFC is proposed, along with an example.

11.Acknowledgements

This research was financially supported by Earthquake Commission Research Foundation (Project 14/U687 “Sliding Hinge Joint Connection with BeSs”). The authors are grateful for this support. The first author PhD studies at the UoA is financially supported through a QuakeCoRE PhD scholarship. This support is much appreciated. A number of this article's figures are drawn by Marie Poirot. This help is appreciated.

Table captions

Table 1. Load distribution along the steel bolt threaded part which is in contact with the nut threads

Table 2. Calculation steps associated with the AFC and SFC bolt installation and post sliding tension loss with and without BeSs

Figure captions

Figure 1) The symmetric friction connection (SFC) with slotted middle plate layout [41] (a) and slotted outer plates layout (b), and the SFC idealized force-displacement behaviour (c)

Figure 2) The rotational slotted bolted connection (RSBC) layout [6]

Figure 3. The sliding hinge joint (SHJ) views (a) front (b) beam cross sectional, (c) back, and (d) 3D

Figure 4. (a) AFC in the bottom flange plate and (b) AFC idealized force-displacement behaviour [41]

Figure 5. AFC idealised bolt deformation, external forces, and bending moment distribution [13]

Figure 6. Surface roughness, waviness, and microscopic high spots on a schematic sliding surface

Figure 7. Four parts of a bolt acting as a set of spring systems in carrying the bolt pretension load

Figure 8. Load distribution along the steel bolt threaded part which is in contact with the nut threads, and the nut threads

Figure 9. Joint plies acting as a set of springs in series: (a) with hardened washer, (b) with BeSs

Figure 10. The equivalent cylinder, QD_{0s}, and qD_{0s} in cylindrical Stress Field "Q factor" approach

Figure 11. The assumed stress field in the frustum approach

Figure 12. (a) Typical cross sectional layout of a Belleville spring (b) BeS acting as a spring

Figure 13. Bilinear hysteresis load-deflection graph of a BeS

Figure 14. Different configurations of BeSs

Figure 15. Ideal linear load-deflection graph of single, series, and parallel BeSs

Figure 16. AFC and SFC joint plies and bolt assemblage spring model: (a) with hardened washer, (b) with BeSs

Figure 17. Dimensions of the HSFG M20 nut (left) and hardened washer (right)

Figure 18) Post-sliding AFC or SFC bolt tension vs: bolt longitudinal plastic deformation while there is ideally no thickness reduction of the plies (left), and thickness reduction of the AFC or SFC plies while there is ideally no bolt longitudinal plastic deformation (right)

Figure 19) Post-sliding bolt tension vs combination of AFC or SFC bolt longitudinal plastic deformation and plies thickness reduction without BeSs (left) and with BeSs (right)

Figure 20) Prying action on the AFC without BeSs or with flattened BeSs (left) and with not flattened BeSs (right)

Figure 21) Variations of the joint forces per bolt including the bolt tension, lower faying force, upper faying force, and total faying force under the prying actions for the cases without BeSs or with flattened BeSs (left), and with not flattened BeSs (right)

Figure 22) The AFC bolt head and nut stable sliding support conditions for the cases without BeSs or with flattened BeSs (left) and with not flattened BeSs providing the self-centering components (right)

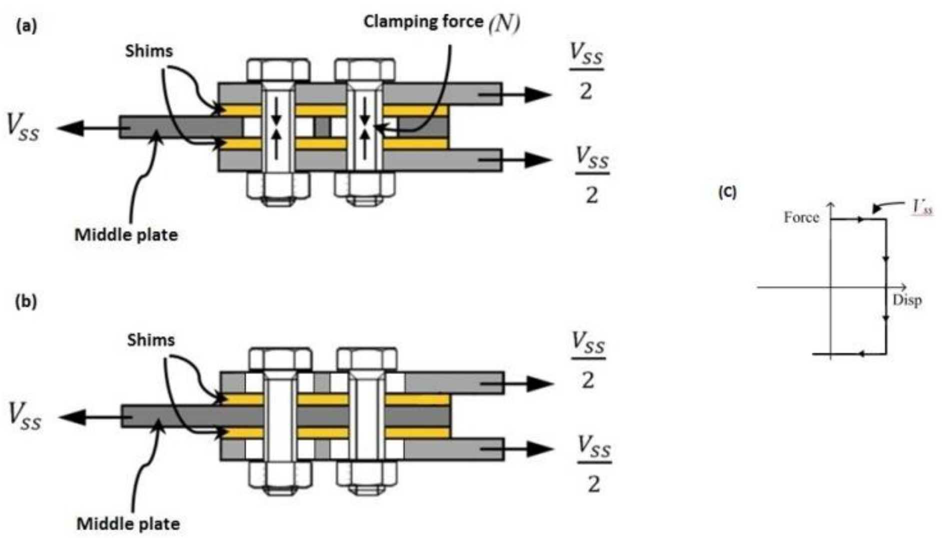

Figure 1) The symmetric friction connection (SFC) with slotted middle plate layout [41] (a) and slotted outer plates layout (b), and the SFC idealized force-displacement behaviour (c)

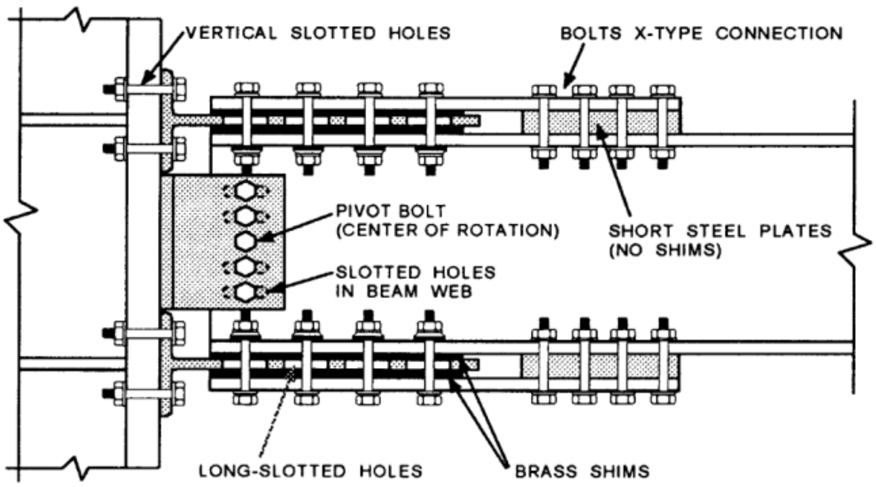

Figure 2) The rotational slotted bolted connection (RSBC) layout [6]

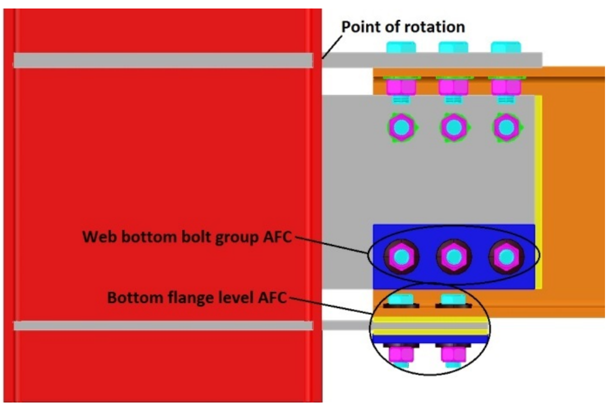

(a)

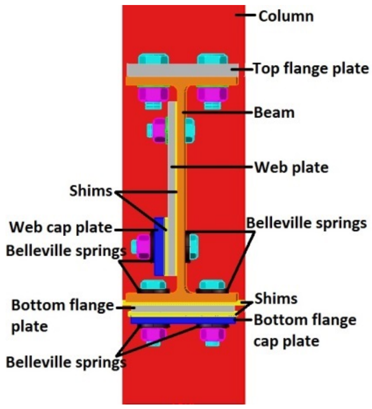

(b)

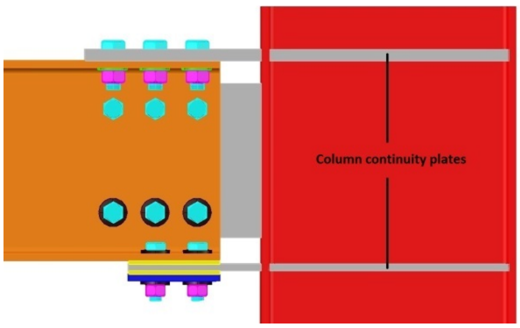

(c)

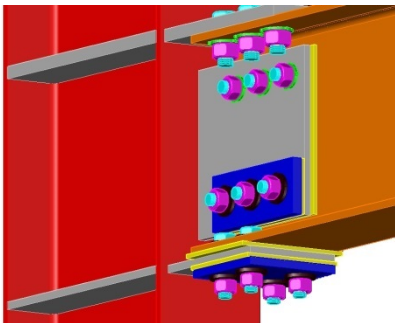

(d)

Figure 3. The sliding hinge joint (SHJ) views (a) front (b) beam cross sectional, (c) back, and (d) 3D

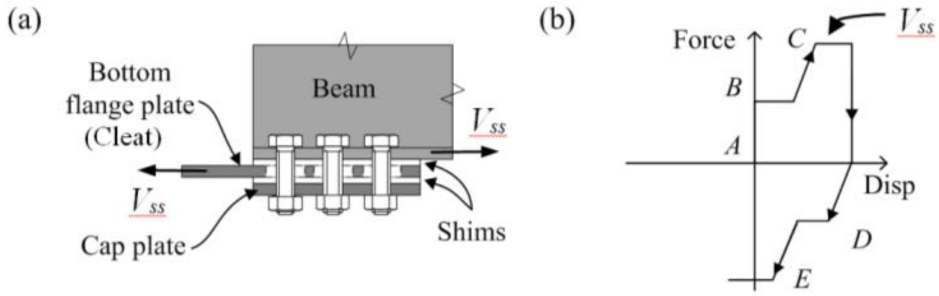

Figure 4. (a) AFC in the beam bottom flange and (b) AFC idealized force-displacement behaviour [41]

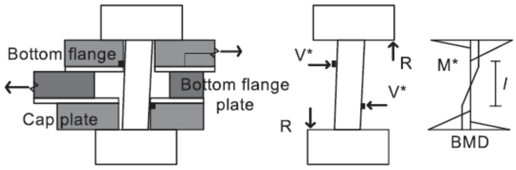

Figure 5. AFC idealised bolt deformation, external forces, and bending moment distribution [13]

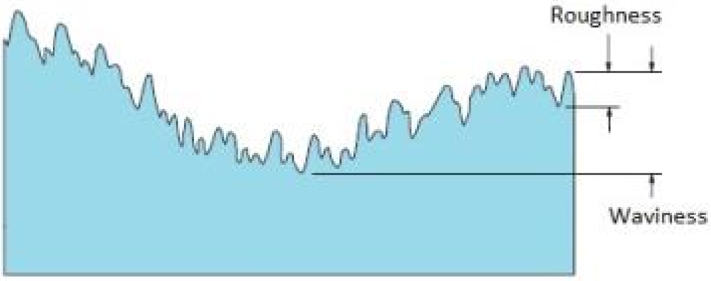

Figure 6. Surface roughness, waviness, and microscopic high spots on a schematic sliding surface

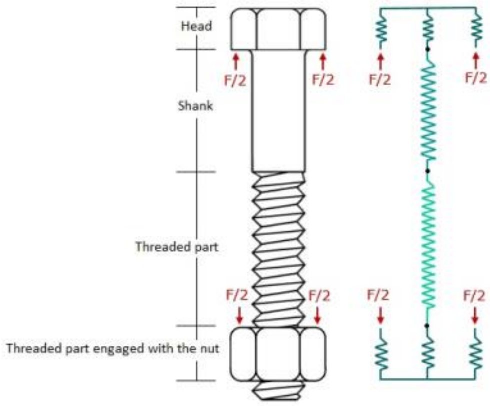

Figure 7. Four parts of a bolt acting as a set of spring systems in carrying the bolt pretension load

Table 1. Load distribution along the steel bolt threaded part which is in contact with the nut threads

Load distribution (% of bolt tension)	31	21.5	14.5	10.5	8	6	5	3.5	0
Distance from the nut underneath (% of the nut height)	0	12.5	25	37.5	50	62.5	75	87.5	100

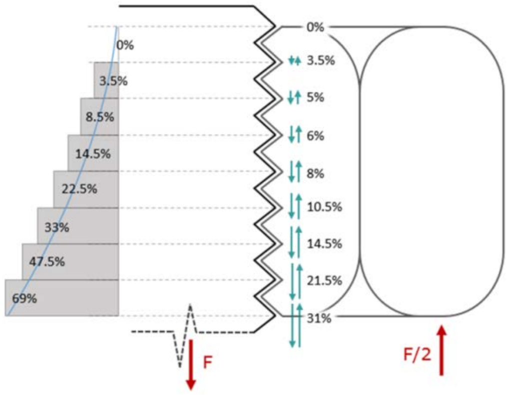

Figure 8. Load distribution along the steel bolt threaded part which is in contact with the nut threads, and the nut threads

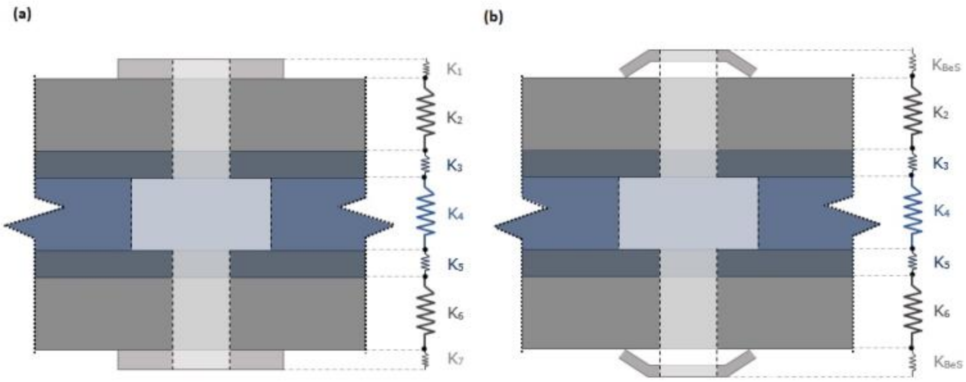

Figure 9. Joint plies acting as a set of springs in series: (a) with hardened washer, (b) with BeSs

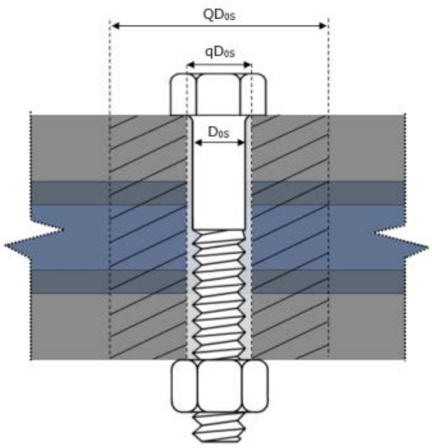

Figure 10. The equivalent cylinder, QD_{0s}, and qD_{0s} in cylindrical Stress Field "Q factor" approach

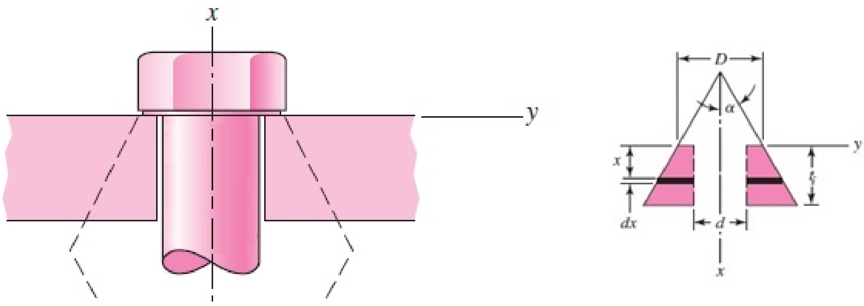

Figure 11. The assumed stress field in the frustum approach

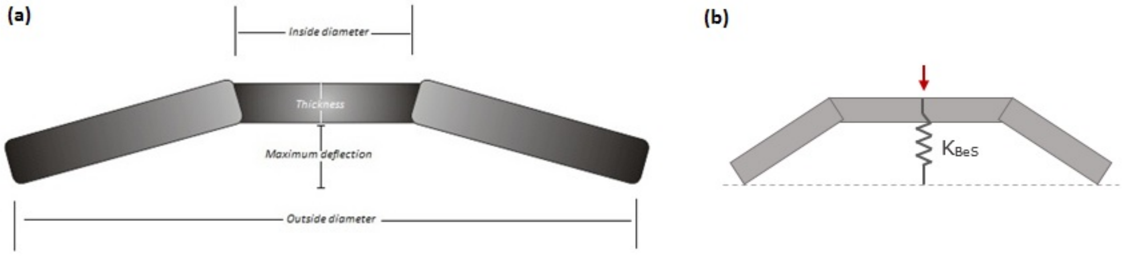

Figure 12. (a) Typical cross sectional layout of a Belleville spring (b) BeS acting as a spring

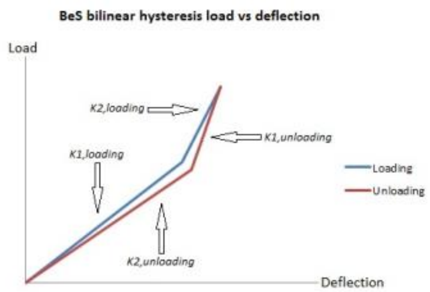

Figure 13. Bilinear hysteresis load-deflection graph of a BeSs

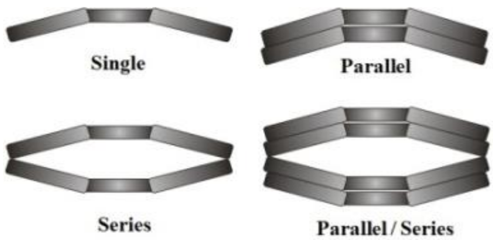

Figure 14. Different configurations of BeSs

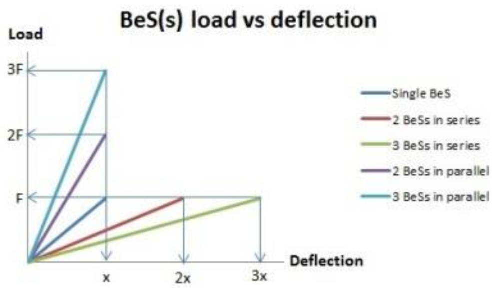

Figure 15. Ideal linear load-deflection graph of single, series, and parallel BeSs

Table 2. Calculation steps associated with the AFC and SFC bolt installation and post sliding tension loss with and without BeSs

Step	Description	Source(s) for calculations
a)	Calculating the stiffness of the plies K_{plies} **(a1)** and hardened washers $K_{hardened\ washer}$ and/or BeS(s) K_{BeS} **(a2)**	Equation 12 and section 5
b)	Calculating the overall stiffness of the plies and hardened washers K_j **(b1)** or overall stiffness of the plies and BeS(s) K_{j-BeS} **(b2)**	Equation 10 and results from **a)**
c)	Calculating the post tightening elastic deformation of the plies and washers ΔL_j or plies Δl_{plies}	Hooke's law and results from **a)** or **b)**
d)	Calculating (A_{0n}/A_{0t}) ratio	Bolt/nut geometry
e)	Calculating the required length of the bolt threaded part between the shank and nut underneath L_{0t} to clamp the plies	Equations 1, 2, 6, and 7, and displacement compatibility
f)	Calculating the required turn of the nut without BeS(s) $\propto_{nut}$ or with BeS(s) $\propto_{nut-BeS}$ to tension the bolt up to the elastic installed bolt tension, if all of the plies, hardened washers and/or BeSs, nut underneath, and bolt head underneath are perfectly in contact, with the bolt tension equal to zero	Displacement compatibility and pitch of the thread.
g)	Calculating the bolt overall stiffness K_{bolt}	Equation 9 and results from **e)**
h)	Calculating the post sliding plies stiffness $K_{plies-ps}$ following the plies' thickness being reduced by the amount of δ_p	Equation 12
i)	Calculating the overall post-sliding stiffness of the joint, i.e. plies and hardened washers K_{j-ps} or plies and BeS(s) $K_{j-ps-BeS}$	Equation 10, results from **h)**, and section 5
j)	Forming two equations two unknowns for post sliding bolt elongation and joint compression following the bolt being perfectly-plastically stretched such that the initial length of the bolt (underneath of the nut to underneath of the head) is increased by the amount of δ_b and the plies overall thickness is reduced by the amount of δ_p	Force equilibrium and displacement compatibility
k)	Calculating the post sliding bolt tension for the case without BeSs $T_{bolt-ps}$, and with BeSs $T_{bolt-ps-BeS}$. These are functions of two variables i.e. δ_b and δ_p.	Hooke's law and results from **j)**

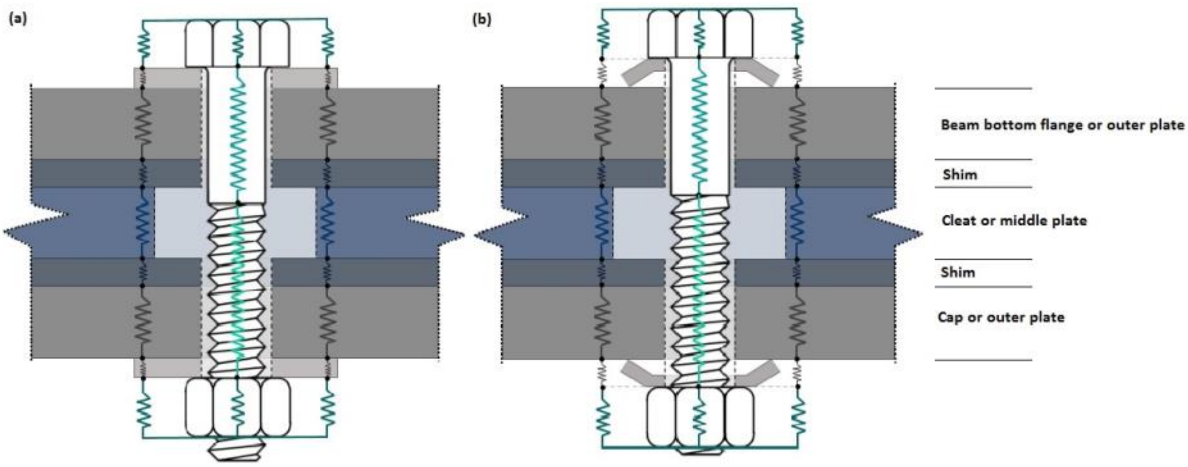

Figure 16. AFC and SFC joint plies and bolt assemblage spring model: (a) with hardened washers, (b) with BeSs

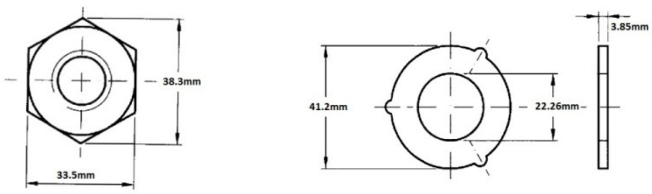

Figure 17. Dimensions of the HSFG M20 nut (left) and hardened washer (right)

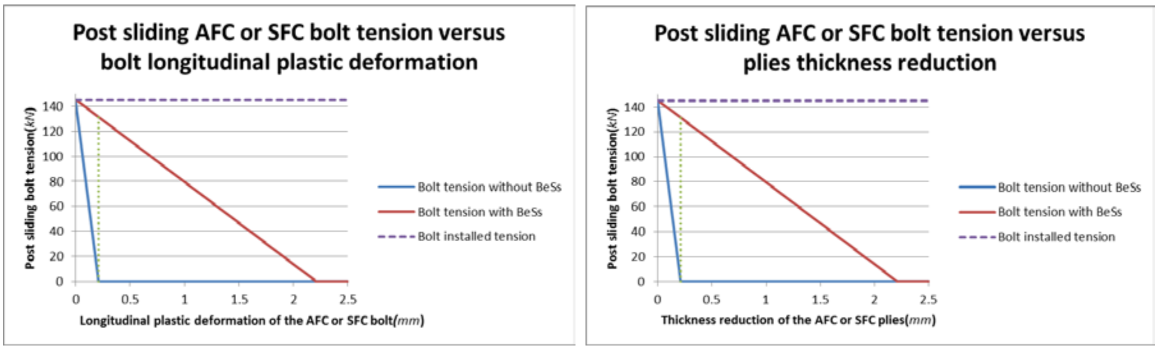

Figure 18) Post-sliding AFC or SFC bolt tension vs: bolt longitudinal plastic deformation while there is ideally no thickness reduction of the plies (left), and thickness reduction of the AFC or SFC plies while there is ideally no bolt longitudinal plastic deformation (right)

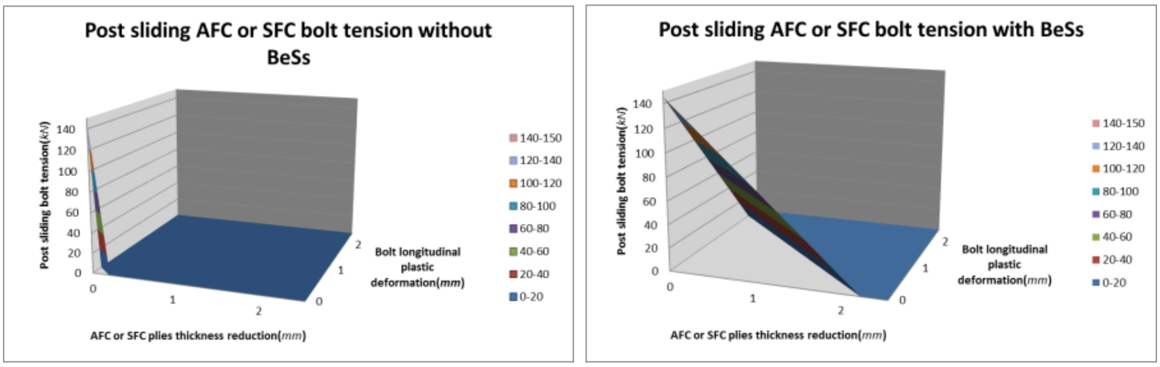

Figure 19) Post-sliding bolt tension vs combination of AFC or SFC bolt longitudinal plastic deformation and plies thickness reduction without BeSs (left) and with BeSs (right)

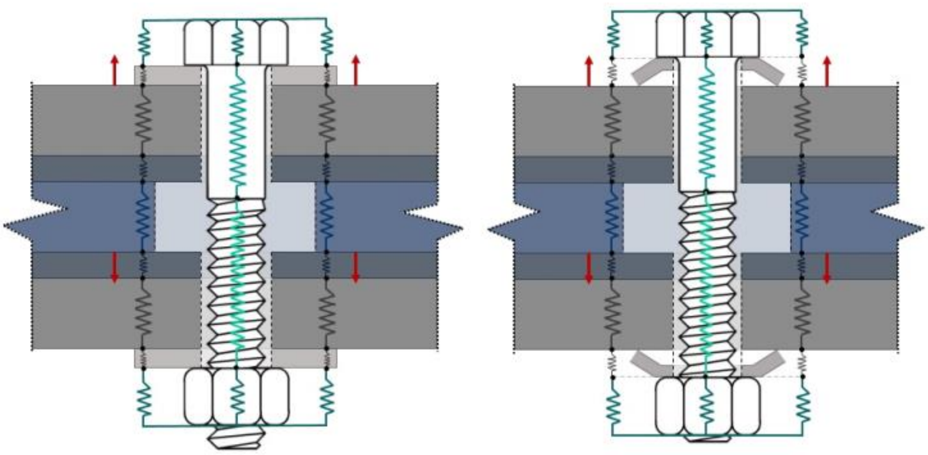

Figure 20) Prying action on the AFC without BeSs or with flattened BeSs (left) and with not flattened BeSs (right)

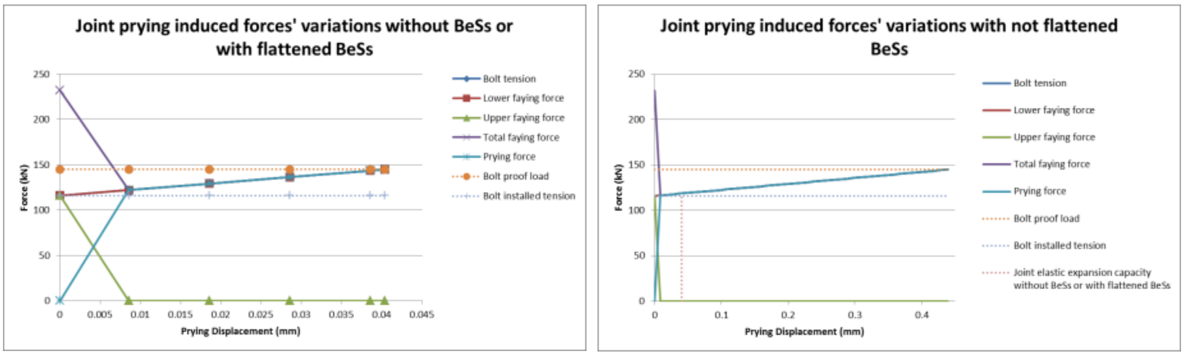

Figure 21) Variations of the joint forces per bolt including the bolt tension, lower faying force, upper faying force, and total faying force under the prying actions for the cases without BeSs or with flattened BeSs (left), and with not flattened BeSs (right)

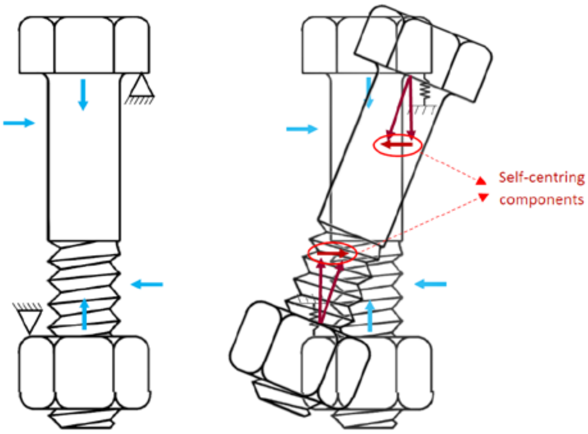

Figure 22) The AFC bolt head and nut stable sliding support conditions for the cases without BeSs or with flattened BeSs (left) and with not flattened BeSs providing the self-centering components (right)

References

1. Hamburger, R.O. and K. Frank. *Performance of Welded Steel Moment Connections - Issues Related to Materials and Mechanical Properties*. in *The Workshop on Steel Seismic Issues*. 1994. USA.
2. Park, R., I.J. Billings, G.C. Clifton, J. Cousins, A. Filiatrault, D.N. Jennings, L.C.P. Jones, N.D. Perrin, et al., *The Hyogo-Ken Nanbu Earthquake of 17 January 1995.* Bulletin of the New Zealand Society for Earthquake Engineering, 1995. **28**(1): p. 100.
3. Engelhardt, M.D., *Ductile Detailing of Steel Moment Frames: Basic Concepts, Recent Developments and Unresolved Issues*, in *XIII Mexican Conference on Earthquake Engineering*2001: Guadalajara, Mexico.
4. Roeder, C., *Connection Performance for Seismic Design of Steel Moment Frames.* Journal of Structural Engineering, 2002. **128**(4): p. 517-525.
5. Khoo, H.H., *Development of the low damage self-centering Sliding Hinge Joint*, in *Department of Civil and Environmental Engineering*2013, University of Auckland: Auckland, New Zealand.

6. Yang, T.-S. and E.P. Popov, *Experimental and Analytical Studies of Steel Connections and Energy Dissipators*, 1995, Earthquake Engineering Research Center: Berkeley, University of California.
7. Clifton, G.C., G.A. MacRae, H. Mackinven, S. Pampanin, and J. Butterworth, *Sliding Hinge Joints and Subassemblies for Steel Moment Frames*, in *The 2007 New Zealand Society for Earthquake Engineering (NZSEE) Annual Technical Conference - Perforrmance by design — can we predict it?*2007: Palmerston North, New Zealand.
8. Pall, A.S., *Limited Slip Bolted Joints - A Device to Control the Seismic Response of Large Panel Structures*, in *Centre for Building Studies*1979, Concordia University: Montreal, Quebec, Canada.
9. Pall, A.S. and C. Marsh, *Response of friction damped braced frames.* Journal of Structural Engineering, 1982. **108**(9): p. 1313-1323.
10. Filiatrault, A. and S. Cherry, *Performance Evaluation of Friction Damped Braced Steel Frames Under Simulated Earthquake Loads.* Earthquake Spectra, 1987. **3**(1): p. 57-78.
11. FitzGerald, T.F., T. Anagnos, M. Goodson, and T. Zsutty, *Slotted Bolted Connections in Aseismic Design for Concentrically Braced Connections.* Earthquake Spectra, 1989. **5**(2): p. 383-391.
12. Kim, H.-J. and C. Christopoulos, *Friction damped posttensioned self-centering steel moment-resisting frames.* Journal of Structural Engineering, 2008. **134**(11): p. 1768-1779.
13. MacRae, G.A., G.C. Clifton, H. Mackinven, N. Mago, J. Butterworth, and S. Pampanin, *The Sliding Hinge Joint Moment Connection.* Bulletin of the New Zealand Society for Earthquake Engineering, 2010. **43**(3): p. 202.
14. Latour, M., V. Piluso, and G. Rizzano, *Experimental analysis on friction materials for supplemental damping devices.* Construction and Building Materials, 2014. **65**: p. 159-176.
15. Grigorian, C.E. and E.P. Popov, *Energy dissipation with slotted bolted connections*, 1994, Earthquake Engineering Research Centre: Berkeley, California.
16. Khoo, H.H., C. Clifton, J. Butterworth, G. MacRae, and G. Ferguson, *Influence of steel shim hardness on the Sliding Hinge Joint performance.* Journal of Constructional Steel Research, 2012. **72**: p. 119-129.
17. Iyama, J., C.Y. Seo, J.M. Ricles, and R. Sause, *Self-centering MRFs with bottom flange friction devices under earthquake loading.* Journal of Constructional Steel Research, 2009. **65**(2): p. 314-325.
18. Tsai, K.C., C.C. Chou, C.L. Lin, P.C. Chen, and S.J. Jhang, *Seismic self-centering steel beam-to-column moment connections using bolted friction devices.* Earthquake Engineering & Structural Dynamics, 2008. **37**(4): p. 627-645.
19. Rojas, P., J. Ricles, and R. Sause, *Seismic performance of post-tensioned steel moment resisting frames with friction devices.* Journal of Structural Engineering, 2005. **131**(4): p. 529-540.
20. Wolski, M., J.M. Ricles, and R. Sause, *Experimental study of a self-centering beam–column connection with bottom flange friction device.* Journal of Structural Engineering, 2009. **135**(5): p. 479-488.
21. Tremblay, R., M. Lacerte, and C. Christopoulos, *Seismic response of multistory buildings with self-centering energy dissipative steel braces.* Journal of Structural Engineering, 2008. **134**(1): p. 108-120.
22. Christopoulos, C., R. Tremblay, H.-J. Kim, and M. Lacerte, *Self-centering energy dissipative bracing system for the seismic resistance of structures: development and validation.* Journal of Structural Engineering, 2008. **134**(1): p. 96-107.
23. Golondrino, J.C., G.A. MacRae, J.G. Chase, G.W. Rodgers, and G.C. Clifton, *Hysteretic Behavior of Symmetrical Friction Connections (SFC) Using Different Steel Grade Shims*, in *10th Pacific Structural Steel Conference*2013: Singapore.

24. Zhu, S. and Y. Zhang, *Seismic analysis of concentrically braced frame systems with self-centering friction damping braces.* Journal of Structural Engineering, 2008. **134**(1): p. 121-131.
25. Loo, W.Y., P. Quenneville, and N. Chouw, *A new type of symmetric slip-friction connector.* Journal of Constructional Steel Research, 2014. **94**: p. 11-22.
26. Leung, H.K., G.C. Clifton, H.H. Khoo, and G.A. MacRae, *Experimental Studies of Eccentrically Braced Frame with Rotational Bolted Active Links*, in *8th International Conference on Behavior of Steel Structures in Seismic Areas (STESSA)*2015: Shanghai, China.
27. Clifton, G.C., *Semi-rigid joints for moment-resisting steel framed seismic-resisting systems*, in *Department of Civil and Environmental Engineering*2005, University of Auckland: Auckland, New Zealand.
28. NZS3404. *Steel structures standard, incorporating Amendments 1 and 2*. 1997/2001/2007. Wellington [N.Z.]: Standards New Zealand.
29. Borzouie, J., G.A. MacRae, J.G. Chase, G.W. Rodgers, and G.C. Clifton, *Experimental studies on cyclic performance of column base weak axis aligned asymmetric friction connection.* Journal of Constructional Steel Research, 2015. **112**: p. 252-262.
30. Borzouie, J., G.A. MacRae, J. Chase, G. Rodgers, and G.C. Clifton, *Experimental Studies on Cyclic Performance of Column Base Strong Axis–Aligned Asymmetric Friction Connections.* Journal of Structural Engineering, 2015. **0**(0): p. 04015078.
31. Golondrino, J.C., R. Xie, G.A. MacRae, G. Chase, G. Rodgers, and C. Clifton, *Braced Frame Using Asymmetrical Friction Connections (AFC)*, in *8th Conference on Behaviour of Steel Structures in Seismic Areas (STESSA)*2015: Shanghai, China.
32. Ramhormozian, S., G.C. Clifton, G.A. Macrae, and H.-H. Khoo, *Improving the seismic behaviour of the Sliding Hinge Joint using Belleville Springs*, in *8th Conference on Behaviour of Steel Structures in Seismic Areas (STESSA)*2015: Shanghai, China.
33. Khoo, H.H., C. Clifton, J. Butterworth, G. MacRae, S. Gledhill, and G. Sidwell, *Development of the self-centering Sliding Hinge Joint with friction ring springs.* Journal of Constructional Steel Research, 2012. **78**: p. 201-211.
34. Tremblay, R., *Seismic behavior and design of friction concentrically braced frames for steel buildings*, 1993, The University of British Columbia.
35. Ferrante Cavallaro, G., A. Francavilla, M. Latour, V. Piluso, and G. Rizzano, *Experimental behaviour of innovative thermal spray coating materials for FREEDAM joints.* Composites Part B: Engineering, 2017. **115**: p. 289-299.
36. Latour, M., V. Piluso, and G. Rizzano, *Free from damage beam-to-column joints: Testing and design of DST connections with friction pads.* Engineering Structures, 2015. **85**: p. 219-233.
37. Ramhormozian, S., G.C. Clifton, D. Cvitanich, S. Maetzig, and G.A. Macrae, *Recent Developments on the Sliding Hinge Joint*, in *New Zealand Society for Earthquake Engineering (NZSEE) Annual Technical Conference - Reducing Risk Raising Resilience*2016: Christchurch, New Zealand
38. Ramhormozian, S., G.C. Clifton, B. Bergen, M. White, and G.A. Macrae, *An Experimental Study on the Asymmetric Friction Connection (AFC) Optimum Installed Bolt Tension*, in *NZSEE Annual Technical Conference and 15th World Conference on Seismic Isolation, Energy Dissipation and Active Vibration Control of Structures*2017: Wellington, New Zealand.
39. Mago, N., *Finite Element Analysis of Sliding Hinge Joint*, 2002, NZ Heavy Engineering Research Association (HERA): Manukau City, New Zealand.
40. Ramhormozian, S., G. Clifton, and G. MacRae. *The Asymmetric Friction Connection with Belleville springs in the Sliding Hinge Joint*. in *New Zealand Society for Earthquake Engineering (NZSEE) Annual Technical Conference, Towards Integrated Seismic Design*. 2014. Auckland, New Zealand.
41. Khoo, H.H., C. Clifton, G. MacRae, H. Zhou, and S. Ramhormozian, *Proposed design models for the asymmetric friction connection.* Earthquake Engineering & Structural Dynamics, 2014.

42. Bickford, J., *Handbook of Bolts and Bolted Joints*. 1998: Taylor & Francis.
43. Ingenieure, V.D., *VDI 2230: Systematic Calculation of High Duty Bolted Joints, Joints with One Cylindrical Bolt*. 1986.
44. Bickford, J., *An Introduction to the Design and Behavior of Bolted Joints, Third Edition, Revised and Expanded*. 1995: Taylor & Francis.
45. Grewal, A. and M. Sabbaghian, *Load distribution between threads in threaded connections.* Journal of pressure vessel technology, 1997. **119**(1): p. 91-95.
46. Sopwith, D., *The distribution of load in screw threads.* Proceedings of the Institution of Mechanical Engineers, 1948. **159**(1): p. 373-383.
47. Miller, D.L., K.M. Marshek, and M.R. Naji, *Determination of load distribution in a threaded connection.* Mechanism and machine Theory, 1983. **18**(6): p. 421-430.
48. Wang, W. and K. Marshek, *Determination of load distribution in a threaded connector with yielding threads.* Mechanism and machine Theory, 1996. **31**(2): p. 229-244.
49. Alkatan, F., P. Stephan, A. Daidie, and J. Guillot, *Equivalent axial stiffness of various components in bolted joints subjected to axial loading.* Finite Elements in Analysis and Design, 2007. **43**(8): p. 589-598.
50. Ito, Y., J. Toyoda, and S. Nagata, *Interface pressure distribution in a bolt-flange assembly.* Journal of mechanical design, 1979. **101**(2): p. 330-337.
51. Wileman, J., M. Choudhury, and I. Green, *Computation of member stiffness in bolted connections.* Journal of mechanical design, 1991. **113**(4): p. 432-437.
52. Brown, M. and B. Durbin, *Guideline for Bolted Joint Design and Analysis: Version 1.0.* Sandia Report, SAND2008-0371, Sandia National Laboratories for United States Dept. of Energy, 2013: p. 12.
53. Pulling, E.M., S. Brooks, C. Fulcher, and K. Miller, *Guideline for Bolt Failure Margins of Safety Calculations*, 2005.
54. Shigley, J.E., R.G. Budynas, and C.R. Mischke, *Mechanical engineering design.* 2004.
55. Musto, J.C. and N.R. Konkle, *Computation of Member Stiffness in the Design of Bolted Joints.* Journal of mechanical design, 2005. **128**(6): p. 1357-1360.
56. Morrow, C. and S. Durbin, *Review of the Scale Factor, Q, Approach to Bolted Joint Design*, 2007: Internal Sandia Memo.
57. F.E.D.S, *Bolted Joint Design*, 2009: Fastenal Engineering and Design Support F.E.D.S.
58. Bhandari, V.B., *Design of Machine Elements*. 2007: Tata McGraw-Hill.
59. Almen, J.O. and A. Laszlo, *The Uniform-Section Disk Spring.* Trans. ASME, 1936. **58**: p. 305-314.
60. Davet, G.P. *Belleville Springs: Keep Joints Tight*. [cited 2016; Available from: http://www.solonmfg.com/springs/faq.cfm.
61. Davet, G.P., *Using Belleville Springs in Sealing Applications to Reduce Fugitive Emissions*, Solon Manufacturing Co.
62. Davet, G.P., *Using Belleville Springs To Maintain Bolt Preload*, 1997, Solon Manufacturing Company: Chardon, Ohio, USA.
63. SCHNORR-manufacturing, *Disc Springs*.
64. Spring-I-Pedia. *Belleville Washers: Stacking*. 2011 2016]; Available from: http://springipedia.com/belleville-washers-stacking.asp.
65. Machine-Design. *Bellevilles put on the squeeze*. [cited 2016; Available from: http://machinedesign.com/technologies/bellevilles-put-squeeze.
66. AS/NZS1252, *High-strength steel bolts with associated nuts and washers for structural engineering*, in *Australia/New Zealand Standard*1996.
67. Ramhormozian, S., G. Clifton, S. Maetzig, D. Cvitanich, and G. MacRae, *Influence of the Asymmetric Friction Connection (AFC) ply configuration, surface condition, and material on the AFC sliding behaviour*, in *New Zealand Society for Earthquake Engineering (NZSEE)*

*Annual Technical Conference, Reducing Risk Raising Resilience*2016: Christchurch, New Zealand.
68. Heistermann, C., *Behaviour of Pretensioned Bolts in Friction Connections: Towards the Use of Higher Strength Steels in Wind Towers*, in *Division of Structural and Construction Engineering – Steel Structures - Department of Civil, Environmental and Natural Resources Engineering*20122, Luleå University of Technology: Sweden.